TECHNICAL REPORT

ISO/IEC TR 20017

First edition
2011-12-15

Information technology — Radio frequency identification for item management — Electromagnetic interference impact of ISO/IEC 18000 interrogator emitters on implantable pacemakers and implantable cardioverter defibrillators

Technologies de l'information — Identification par radiofréquence pour la gestion des objets — Impact des interférences électromagnétiques des émetteurs d'interrogateurs de l'ISO/CEI 18000 sur les stimulateurs cardiaques et les défibrillateurs implantables

Reference number
ISO/IEC TR 20017:2011(E)

ISO copyright office
Case postale 56 • CH-1211 Geneva 20
Tel. + 41 22 749 01 11
Fax + 41 22 749 09 47
E-mail copyright@iso.org
Web www.iso.org

Published in Switzerland

Contents

Page

Foreword iv
Introduction v
1 Scope 1
2 Normative references 1
3 Terms and definitions 1
4 Abbreviated terms 2
5 The need for EMC between RFID and implanted medical devices 3
6 EMI studies 3
6.1 General 3
6.2 FDA/AAMI study 1 3
6.3 FDA/AAMI study 2 3
6.4 Report of Ministry of Internal Affairs and Communications of Japan 4
6.5 JAISA/Hokkaido-University study 5
7 Differences in results 5
8 Need for comprehensive test methodologies 7
Annex A (informative) **JAISA/Hokkaido-University study** 8
Bibliography 53

Foreword

ISO (the International Organization for Standardization) and IEC (the International Electrotechnical Commission) form the specialized system for worldwide standardization. National bodies that are members of ISO or IEC participate in the development of International Standards through technical committees established by the respective organization to deal with particular fields of technical activity. ISO and IEC technical committees collaborate in fields of mutual interest. Other international organizations, governmental and non-governmental, in liaison with ISO and IEC, also take part in the work. In the field of information technology, ISO and IEC have established a joint technical committee, ISO/IEC JTC 1.

International Standards are drafted in accordance with the rules given in the ISO/IEC Directives, Part 2.

The main task of the joint technical committee is to prepare International Standards. Draft International Standards adopted by the joint technical committee are circulated to national bodies for voting. Publication as an International Standard requires approval by at least 75 % of the national bodies casting a vote

In exceptional circumstances, when the joint technical committee has collected data of a different kind from that which is normally published as an International Standard ("state of the art", for example), it may decide to publish a Technical Report. A Technical Report is entirely informative in nature and shall be subject to review every five years in the same manner as an International Standard.

Attention is drawn to the possibility that some of the elements of this document may be the subject of patent rights. ISO shall not be held responsible for identifying any or all such patent rights.

ISO/IEC TR 20017 was prepared by Joint Technical Committee ISO/IEC JTC 1, *Information technology*, Subcommittee SC 31, *Automatic identification and data capture techniques*.

Introduction

In *The Joy of Science* (2001), Robert Hazen notes the definition of science and the scientific method

— Science is a way of knowing about the natural world based on reproducible observations and experiments.

— The idealized scientific method is a cyclic process of inquiry based on observations, synthesis, hypothesis, and predictions that lead to more observations. At the centre of this idealized cycle there is always a paradigm — a prevailing system of expectations about the natural world.

This scientific method can be visualized in Figure 1, below.

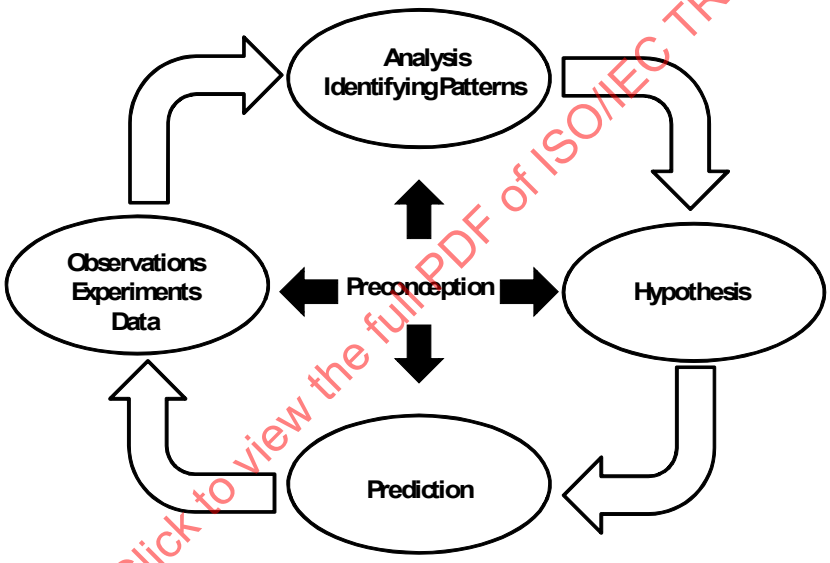

Figure 1 — The Scientific Method

In the world of radio frequency identification there have been numerous applications of this scientific method that have not always yielded reproducible observations.

In the *Journal of the American Medical Association* (JAMA), June 25, 2008—Vol 299, No. 24, Remko van der Togt, MSc, Erik Jan van Lieshout, MD, Reinout Hensbroek, MSc, E. Beinat, PhD, J. M. Binnekade, PhD, and P. J. M. Bakker, MD, PhD [47][1)]. reported that “In 123 EMI tests (3 per medical device), RFID induced 34 EMI incidents: 22 were classified as hazardous, 2 as significant, and 10 as light. The passive 868-MHz RFID signal induced a higher number of incidents (26 incidents in 41 EMI tests; 63%) compared with the active 125-kHz RFID signal (8 incidents in 41 EMI tests; 20%); difference 44% (95% confidence interval, 27%-53%; P<0,001). The passive 868-MHz RFID signal induced EMI in 26 medical devices, including 8 that were also affected by the active 125-kHz RFID signal (26 in 41 devices; 63%). The median distance between the RFID reader and the medical device in all EMI incidents was 30 cm (range, 0.1-600 cm).”

1) Square bracket references can be found in the Bibliography to this Technical Report.

Yet another publication from BlueBean noted a study of radio frequency identification (RFID) testing that was completed on March 10, 2008 at Community North Hospital, Indianapolis, Indiana. This study determined that RFID systems, including near and far field antennas and passive tags, did not influence the performance of commonly used medical devices such as physiological monitors and intravenous pumps.

Would either of these studies be scientific fraud because their experiments yielded different results? Or would it be more likely that different makes and models of RFID interrogators were tested? Or were different makes and models of clinical equipment tested? Or were there variations in both input variables?

In reality, there are multiple studies and there is not agreement between the studies. The differences between the studies are most likely based on different test protocols and different devices tested. The science of implanted devices is one of constant improvement and today's devices are likely to exhibit significantly different results from those used in this test.

This Technical Report looks at the various public reports on the electromagnetic compatibility between RFID interrogators, implantable cardiac pacemakers (pacemakers), and implantable cardioverter defibrillators (ICDs). This Technical Report further recommends the development of a uniform testing protocol and a repository of test results from experiments using those test protocols.

Information technology — Radio frequency identification for item management — Electromagnetic interference impact of ISO/IEC 18000 interrogator emitters on implantable pacemakers and implantable cardioverter defibrillators

1 Scope

This Technical Report presents a test method and results for the evaluation of ISO/IEC 18000 radio frequency identification (RFID) interrogator electromagnetic interference (EMI) on implantable pacemakers and implantable cardioverter defibrillators.

2 Normative references

The following referenced documents are indispensable for the application of this document. For dated references, only the edition cited applies. For undated references, the latest edition of the referenced document (including any amendments) applies.

ISO 14708-1, *Implants for surgery — Active implantable medical devices — Part 1: General requirements for safety, marking and for information to be provided by the manufacturer*

ISO 14708-2, *Implants for surgery — Active implantable medical devices — Part 2: Cardiac pacemakers*

ISO/IEC 19762-1, *Information technology — Automatic identification and data capture (AIDC) techniques — Harmonized vocabulary — Part 1: General terms relating to AIDC*

ISO/IEC 19762-3, *Information technology — Automatic identification and data capture (AIDC) techniques — Harmonized vocabulary — Part 3: Radio frequency identification (RFID)*

ISO/IEC 19762-4, *Information technology — Automatic identification and data capture (AIDC) techniques — Harmonized vocabulary — Part 4: General terms relating to radio communications*

ANSI/AAMI/IEC 60601-1-2:2007, *Medical electrical equipment — Part 1-2: General requirements for basic safety and essential performance — Collateral standard: Electromagnetic compatibility — Requirements and tests*

AAMI TIR18:2010, *Guidance on electromagnetic compatibility of medical devices in healthcare facilities*

ANSI/AAMI PC69, *Active implantable medical devices — Electromagnetic compatibility — EMC test protocols for implantable cardiac pacemakers and implantable cardioverter defibrillators*

3 Terms and definitions

For the purposes of this document, the terms and definitions given in ISO/IEC 19762-1, ISO/IEC 19762-3, ISO/IEC 19762-4, AAMI TIR18:2010, ANSI/AAMI PC69:2007, ANSI/AAMI/IEC 60601-1-2, ISO 14708-1, and ISO 14708-2 apply.

4 Abbreviated terms

Acronym, abbreviation	Description
AAI	Atrial Atrial Inhibited
AAMI	Association for the Advancement of Medical Instrumentation
AIMD	active implantable medical device
ARIB	Association of Radio Industries and Businesses
CRT-D	cardiac resynchronization therapy-defibrillator
CRT-P	cardiac resynchronization therapy-pacemaker
CW	continuous wave
DDDR	A-V sequential Atrial/Ventricular inhibited, triggered with rate modulation
ECG	electrocardiogram
EIRP	effective isotropic radiated power
EMC	electromagnetic compatibility
EMF	electromagnetic fields
EMI	electromagnetic interference
FCC	Federal Communications Commission
FDA	Food and Drug Administration
FDTD method	finite difference time domain method
FHSS	frequency hopping spread spectrum
HF	high frequency (3~30 MHz, for RFID; 13,56 MHz)
ICD	implantable cardioverter defibrillator
JAISA	Japan Automatic Identification Systems Association
MIC	Ministry of Internal Affairs and Communications
MID	maximum interference distance
RFID	radio frequency identification
UHF	ultra-high frequency (300 MHz to 3 GHz, for RFID in this Technical Report; 860-960 MHz)
VVI	Ventricular Ventricular Inhibited

5 The need for EMC between RFID and implanted medical devices

Increasingly, the market is witnessing an increased in the use of wireless technology in health care settings. Such technology includes wireless local area networks and radio frequency identification (RFID). Additionally, medical devices and clinical instruments are incorporating wireless technology as part of their communications. The growth of wireless technology in health care makes the presumption that its use is benign in such settings. RFID can be used to manage inventory, track items simplify patient billing data collection, and actually improve patient safety by ensuring that the right drug, procedure, or therapy is introduced to the right patient and at the right time.

A 1997 Study by Hayes, et al, *Interference with Cardiac Pacemakers by Cellular Telephones* [28], reported

Use of telephones in the normal position — at the ear — was associated with the lowest incidence of interference of any position tested and did not result in any clinically significant interference. Placement of the telephone over the pacemaker should be avoided. While the telephone is on, it should not be carried in a pocket over or close to the pacemaker.

Such increased prevalence of wireless technology in health care settings and the general population, combined the growth in the population of individuals with implanted devices makes imperative the need for electromagnetic compatibility (EMC) between the wireless technology and the implanted device.

6 EMI studies

6.1 General

There are multiple published studies on the experimental results of measuring the EMI on implantable pacemakers and ICDs due to RFID interrogators [19], [32]~[38]. The data that this TR (Annex A) presents do not necessarily show the same EMI performance as other reports. The reasons for the data discrepancies among those reports include the differences of the active implantable medical devices (AIMDs) tested and RFID interrogator transmission parameters such as carrier frequency, continuous/intermittent mode, modulation schemes, etc. Details of EMI results of those reports are summarized below.

6.2 FDA/AAMI study 1

International Journal Radio Frequency Identification Technology and Applications, Vol. 1, No.3, 2007, *Electromagnetic compatibility of pacemakers and implantable cardiac defibrillators exposed to RFID readers*, Seth J. Seidman, Paul S. Ruggera, Randall G. Brockman, Brian Lewis and Mitchell J. Shein [37] reported a reaction in 6% of the pacemakers tested at 915 MHz, 18% of the pacemakers tested at 13,56 MHz, and 83% of those tested at 134 kHz. For ICDs they reported reactions in 0% at 915 MHz, 11% at 13,56 MHz, and 71% of those tested at 134 kHz.

Here, EMI event was estimated by monitoring the oscilloscope for any change in the AIMD's output signal. The RFID interrogators specified by ISO/IEC 11785 for LF, ISO/IEC 15693 for HF, and ISO/IEC 18000-6, Type C for 915 MHz were used.

This study is subject to copyright by Inderscience, so it is not reproduced here. It can be found at: http://www.inderscience.com/search/index.php?action=record&rec_id=15848&prevQuery=&ps=10&m=or

6.3 FDA/AAMI study 2

In In Vitro Tests Reveal Sample Radio Frequency Identification Readers Inducing Clinically Significant Electromagnetic Interference to Implantable Pacemakers and Implantable Cardioverter Defibrillators, published in Heart Rhythm Journal Seth J. Seidman, Randall Brockman, Brian Marc Lewis, Joshua Guag, Mitchell J. Shein, Wesley J. Clement, James Kippola, Dennis Digby, Catherine Barber, and Dan Huntwork [38] reported.

A reaction was observed in 174 out of 260 pacemaker tests while being exposed to LF RFID readers (67%). Class I reactions were observed in 102 tests (39%), class III reactions were observed in 72 tests (28%), and 86 of the tests saw no effect (33%). While being exposed to HF RFID readers a reaction was observed in 20 out of 335 pacemaker tests (6%). Class I reactions were observed in 12 tests (4%), class III reactions were observed in 8 tests (2%), and 315 tests saw no effect (94%). There were no reactions (0 out of 112) observed for pacemakers being exposed to either of the two UHF RFID readers.

For ICDs, a reaction was observed in 69 out of 146 tests while being exposed to LF RFID readers (47%). Class I reactions were observed in 62 tests (46%), class III reactions were observed in 7 tests (5%), and 77 of the tests saw no effect (53%). While being exposed to HF RFID readers a reaction was observed in 2 out of 178 ICD tests (1%). Both reactions were class III reactions. There were no reactions (0 out of 60) observed for ICDs being exposed to either of the two UHF RFID readers.

While being exposed to LF RFID, a reaction was observed for 67% of all pacemaker tests (maximum distance 60 cm) and 47% of all ICD tests (maximum distance 40 cm). During HF RFID exposure, a reaction was observed for 6% of all pacemaker tests (maximum distance 22,5 cm) and 1% of all ICD tests (maximum distance 7,5 cm). For both pacemakers and ICDs, no reactions were observed during exposure to UHF RFID or continuous-wave RFID. Pacemakers and ICDs were most susceptible to modulated LF RFID readers.

Here, EMI event was estimated based upon 3 classes of clinical significance defined by Hayes et al. [28]. The RFID interrogators specified by ISO/IEC 11785 for LF, ISO/IEC 18000-3, Mode 1 for HF, and ISO/IEC 18000-6, Type C for 915 MHz were used.

This study is subject to copyright by *Heart Rhythm Journal*, so it is not reproduced here. It can be found at:

http://www.heartrhythmjournal.com/article/S1547-5271%2809%2901146-1/abstract

6.4 Report of Ministry of Internal Affairs and Communications of Japan

In March 2007, the Japanese Ministry of Internal Affairs and Communications published its *Study Report on the Effect of Radio Waves on Medical Devices* [19], which begins

We are moving toward the creation of a ubiquitous network society that makes it possible to connect "anytime, from anywhere, with any device, by anyone" and allows us free access to information (FY 2006 Information and Communications White Paper, MIC). As a result, the use of radio waves has increased dramatically and is becoming an essential part of daily life. At the same time, the effects of radio waves on pacemakers and other medical equipment has become a broad public concern. Thus, it is important to provide the public with information based on the latest studies and relieve their concern in this regard.

The question of the effects of radio waves on medical equipment was first raised in March 1997, in a paper entitled Guidelines on the Use of Radiocommunication Equipment such as Mobile Phones and Safeguards for Electronic Medical Equipment, written by the Electromagnetic Compatibility Conference (currently the Electromagnetic Compatibility Conference Japan). Later, the MIC conducted a study of the effects of radio waves on implantable cardiac pacemakers.

A series of studies were conducted in the ensuing years: Effects of Mobile Telephones (2001), Wireless Card Systems and Electronic Article Surveillance (EAS) Devices (2002); Effects of Gate and Handheld RFID Devices, EAS Devices, and Wireless LAN Equipment (2003); and Effects of RFID Devices and Mobile Telephones. Then, in August 2005 the results of these studies were announced and became the basis of policy advices. A new study was conducted in 2005 on the effects of radio wave emissions from mobile telephones on implantable cardiac pacemakers, based on a study of the effects of mobile terminals as well as the results of other studies, using both domestic and international standards.

RFID devices that use the UHF band were introduced into the market in fiscal 2005. The penetration of the mobile telephone has also been dramatic, and there have been many new models and types introduced into the market since the last study in fiscal 2005. In the world of implantable cardiac pacemakers as well, there have been many new devices approved for use. There is also a need for a new investigation into whether an electromagnetic environment is being maintained for the safe use of these RFID devices and mobile telephone terminals.

As a result, the Ministry of Internal Affairs and Communications (MIC) contracted the Association of Radio Industries and Businesses (ARIB) to conduct a study on the effects of emissions from RFID devices and mobile telephones on implantable cardiac pacemakers and implantable cardioverter defibrillators.

The Association of Radio Industries and Businesses established the Study Group on the Effects of Radio Waves on Medical and Other Equipment to conduct a study of the radio waves emitted from mobile telephones and their effects on implantable cardiac pacemakers with the purpose of applying the results to amending existing policy. This study group received the typical devices being used in Japan today from the Pacemaker Committee, the Japan Automatic Identification Systems Association, and telecommunications carriers, and conducted a study on the effects of radio waves on medical and other equipment. They also conducted electro-magnetic interference tests to examine the effects of radio waves emitted from RFID devices and mobile telephones on implantable cardiac pacemakers, and they performed an analysis of the effects of the radio waves from RFID devices on implantable cardiac pacemakers.

6.5 JAISA/Hokkaido-University study

In this study, since an EMI event is estimated based upon an engineering perspective, for example whether or not any change in the pacing behaviour occurred, the EMI experimental results shown by this study do not necessarily reflect direct risk to patients. The clinical significance estimations remain to be discussed in future studies.

A reaction was observed in 161 out of 450 pacemaker tests while being exposed to LF RFID interrogators (29,3%). While being exposed to HF RFID interrogators a reaction was observed in 39 out of 912 pacemaker tests (4,3%). There were no reactions (0 out of 304) observed for pacemakers being exposed to 2,45 GHz RFID interrogators. While being exposed to UHF RFID interrogators a reaction was observed in 40 out of 952 pacemaker tests (4,2%).

For ICDs, a reaction was observed in 6 out of 82 tests while being exposed to LF RFID interrogators (7,3%). While being exposed to gate-type HF RFID interrogators a reaction was observed in 1 out of 25 ICD tests (4%). No reaction was observed when handheld or stationary type HF RFID interrogators were tested. There were no reactions observed for ICDs being exposed to either UHF or 2,45 GHz RFID interrogators.

While being exposed to LF RFID, a reaction was observed at the maximum distance of 16 cm for pacemakers and at the maximum distance of 4 cm for ICDs. During HF RFID exposure, a reaction was observed at the maximum distance of 23 cm for pacemakers and at the maximum distance of 3 cm for ICDs. During UHF RFID exposure, a reaction was observed at the maximum distance 75 cm with one pacemaker but other pacemakers all showed distances less than 20 cm.

Here, the RFID interrogators specified by ISO/IEC 18000-2 Type A for LF, 18000-3 Mode 1 for HF, 18000-4 Mode 1 for 2,45 GHz and 18000-6 Type C for 953 MHz were used.

Details are described in Annex A.

7 Differences in results

The principal differences between the FDA/AAMI studies [37], [38] and that contained within Annex A of this Technical Report are the pacemakers and ICDs tested, different RF regulations placed on RFID interrogators, and a different (although similar) test methodology.

The implantable pacemakers and ICDs studied in the FDA/AAMI study 2 were all manufactured between 2004 and 2008 and provide a reasonable sample of presently implanted devices in the U.S. The majority of devices tested in Annex A of this TR were approved for use in Japan prior to 2004 and many (30%) implantable pacemakers were approved prior to 1999 and represented a reasonable sample of devices implanted in Japan. Manufacturers began implementing capacitive feed-through filters in the late 1990s and it is likely that some devices tested in Annex A of this Technical Report did not include this particular filtering technique. Additionally, newer devices tend to have improved EMI filtering techniques as better technology becomes available.

There are different regulations placed on RFID interrogators in Japan and the U.S. UHF (915 MHz) interrogators used in the U.S. follow FCC Rule 15.247 [7], which use a frequency-hopping scheme with a maximum peak conducted output power of 1 W (less than or equal to 4 W EIRP). Japan, on the other hand, follows ARIB STD-T89 [11] and operates continuously at the same frequency with the same power limit. The field strength of any emissions within the band 13,553-13,567 MHz cannot exceed 15 848 μV/m at 30 m in the U.S. (per FCC Rule 15.225) [8] and 47 544 μV/m at 10 m in Japan (ARIB STD-T 82) [12]. LF interrogators (125-134 kHz) in the U.S. follow FCC Rule 15.209 [9] and have a maximum allowed field strength of 19,2-17,9 microvolts/meter at 300 meters which is similar to Japan's regulation (Enforcement regulations of Radio Law, Article 44-1-2 (1)) [14] of 15 μV/m at 382-356 m.

Although the test methodologies were similar, there are some significant differences that could also help explain the different results. The FDA/AAMI study 2 duplicated an anatomical layout in shape and used an area of 225 cm^2 for the lead system. The lead system in this TR was a circular loop originally proposed by Irnich [21] of 573 cm^2 (2,5 times larger than that of the FDA/AAMI study 2). Irnich originally proposed 573 cm^2 [21], but more recent studies [22] confirm that 225 cm^2 is more representative for a large human. ANSI/AAMI PC69 measured the average left pectoral geometric loop area to be 191 cm^2 for pacemakers (232 cm^2 for ICDs) and the worst case is 319 cm^2. Additionally the pacemakers and ICDs were set to AAI and VVI during this TR and were set to DDDR[2)] for the FDA/AAMI study 2.

With regard to ISO/IEC 18000-2 (~135 kHz) RFIDs, contrary to the results reported in Annex A of this TR, other MIDs were measured using the same kind of experiments, as reported in the FDA/AAMI study 2 [38]. The MID differences in this frequency range can also be attributed to the pulse repetition rate of RFID interrogators used in the experiments. In the FDA/AAMI report [38], pulse repetition was set from 4 Hz to 25,8 Hz, while in Annex A of this TR, the default setting was continuous transmission, which lessens the EMI on AIMDs to a greater extent than low-frequency pulsed transmission.

With regard to ISO/IEC 18000-6 (UHF, 4 W EIRP) test results, the worst MID of 75 cm was measured for one pacemaker. An earlier FDA/AAMI study (FDA/AAMI study 1) [37] found only one device to be affected at UHF, and this was an older device that did not have feedthrough filters. In the more-recent FDA/AAMI study 2 [38] all devices tested had feedthrough filters and no effects were observed for UHF interrogators. There is the possibility that the EMI observed at UHF in Annex A of this TR was from a pacemaker that did not include a feedthrough filter.

The FDA/AAMI tests were conducted on pacemakers manufactured in the U.S. Japan does not manufacture pacemakers or ICDs and its tests were conducted on medical devices from many countries.

2) NOTE The terms "DDDR" is a common code for pacemakers and ICDs and means "A-V sequential Atrial/Ventricular inhibited, triggered with rate modulation".

The first letter signifies the chamber paced. V means Ventricle, A is Atrium, D is both or Dual, O is none and occasionally S is used by some manufacturers to mean Single.

The second letter indicates the chamber that is sensed (the ICD/ pacemakers detection of electrical activity).

The third letter indicates the pacers response to sensing; T means it will trigger pacing, I means it will inhibit pacing, D means it will do both inhibiting and triggering, and O means none.

The fourth letter is for programmability functions—Rate responsiveness. P is simple Programmable; M is Multiprogrammable; C is Communicating functions (telemetry); and R is Rate Responsive. If a fourth letter is present it is usually rate responsive.

Therefore, a pacemaker or ICD that is DDDR means the pacemaker is pacing electrical activity in both the atrium and the ventricle and it is sensing activity in both the atrium and the ventricle. When it senses an event it will either trigger a response or inhibit pacing and the rate is responsive (the pacing rate will change in response to sensors that detect changes in metabolic needs to increase the cardiac output).

8 Need for comprehensive test methodologies

All studies, save one — BlueBean — have indicated some EMC issues between RFID equipment and medical devices and clinical equipment. Some types of RFID appear less likely to cause interference than others. Consequently, it is incumbent upon all medical device and clinical equipment manufacturers, RFID equipment manufacturers, and the standards community to well identify the type and extent of interactions. Ultimately, it must be ascertained what the type and extent of interactions can be expected with various combinations of RF emitters and medical devices.

It must also be remembered that each medical device and RF emitter may have different modes of operation that must be addressed. Comprehensive test plans must be created for the testing of this equipment. It is suggested that a project be developed between IEC TC 106 (Electromagnetic fields in the human environment), IEC Subcommittee 62A (Common aspects of electrical equipment used in medical practice), ISO TC 150 (Implants for surgery)/SC 6 (Active implants), and JTC 1/SC 31/WG 4 to investigate these interactions against a common test procedure, torso model, and measurement equipment.

Annex A
(informative)

JAISA/Hokkaido-University study

A.1 Introduction

Several current reports indicate that various electric or electronic devices occasionally may cause malfunctions in active implantable medical devices (AIMD) such as implantable cardiac pacemakers and cardioverter defibrillators (ICDs) through electromagnetic coupling (interference) [15]~[42]. One well-known example is the microwave electromagnetic interference (EMI) created by active cellular phones [16]~[20], [23]~[31]. Some reports have experimentally confirmed that some radio frequency identification (RFID) interrogators might trigger an AIMD malfunction [16], [18]~[20], [22], [32]~[38]. Among them, a Food and Drug Administration (FDA)/Association for the Advancement of Medical Instrumentation (AAMI) report concluded that the clinical risk is low [38]. On the other hand, Japan Automatic Identification Systems Association (JAISA)/Hokkaido-University report shows partially different results. It is probable that the inconsistencies are mainly due to the differences of the devices tested in both experiments. Any standard methodology for evaluating the EMI from RFID interrogators on AIMDs is not available at present, which recognizes a consistency. However, this technical paper provides fundamental information that can be used when investigating or decreasing EMI risk, which is currently needed in present situations.

The observed characteristics of the EMI were shown to depend upon the transmission radio wave specifications, the antenna performance of the interrogator, AIMD type, and AIMD operation mode setting. The typical cases indicate that the EMI is most likely to occur directly in front of the interrogator antenna.

This Annex describes the technologies needed to implement experimental EMI evaluation methods and a method of mitigating the EMI from RFID interrogators on AIMDs. Some experimental evaluation results for typical devices are also presented. In this report, since an EMI event is estimated based upon an engineering stand point, for example whether or not any change in the pacing behaviour occurred, the EMI experimental results shown by this report do not necessarily reflect direct risk to patients. The clinical significance estimations remain to be discussed in future studies.

A recent issue of interest is the possibility of an AIMD that includes a low-power radio transmitter/receiver [44]. This suggests the possibility of reverse EMI, from this type of AIMD on RFID systems, which is not considered by this technical report.

Overview of the EMI characteristics;

The strength of the electromagnetic fields (EMF) created by an RFID interrogator usually decreases with distance from the antenna of the interrogator, which means that the EMF gets stronger as the distance becomes shorter. In most cases, the fundamental relationship can be approximated by free-space attenuation equations.

When an AIMD patient is close to an RFID interrogator antenna, the EMF strength of the interrogator's signal may be large enough to cause some EMI on AIMD operation through the penetration of EMF or the current induced in the AIMD. The basic EMI mechanism is such that the EMF penetration components are detected by nonlinear characteristics of an internal circuit of AIMD (envelope detection) and when the detected signal is similar to any of physiological signals of a few Hz to several hundred Hz and get over the threshold, the AIMD malfunctions could occur [25], [45], [46]. On the other hand, CW or CW-like signals (i.e. frequency modulation and phase modulation) basically generate very little low frequency noises through envelope detection.

This electromagnetic phenomenon depends upon not only the separation distance of the antenna, but also interrogator emission power, and pulse repetition rather than amplitude modulation depth, its antenna's transmission characteristics including polarization scheme, and AIMD type and operation, its lead length and geometry, and so on [19], [25], [32]~[40]. Further investigations are required on the relationships between EMI and these parameters to develop a representative test protocol.

Experimental investigations have confirmed that such EMI shows a reversible and transient response. These effects can be prevented by keeping the AIMD patient from entering the EMI risk zone around the interrogator [16]~[20], [22], [32]~[40].

It is important to estimate the EMI risk zone (with regard to an AIMD) for each type of RFID interrogator in the free-space condition by means of reliable experimental investigations. In this technical report, this zone is identified as the maximum interference distance (MID), the greatest separation distance between the AIMD and RFID interrogator to have any observed possibility of EMI on AIMD operation. The alternative to the in-vitro approach is the in-vivo technique. Since the former is infinitely more flexible in terms of the variety of AIMDs that can be tested and the setting of their operation parameters, as well as offering better test repeatability and safety, only in-vitro measurement setups using a human torso equivalent phantom model are employed.

Mitigation of malfunction risk due to EMI;

As precautionary measures, some safety information and guidance notes have been released on EMI in AIMDs and other medical devices [16]~[20], [27]. Also, guidelines on the separation distance between AIMDs and cellular phones such as 6-inch or 22-cm have been developed and announced as a prompt and practical countermeasure to avoid the EMI risk when using cellular phones [16]~[19], [27]. A more effective approach to improving AIMD immunity would be, as one example, to improve EMI mitigation filters to AIMD input circuits [29]. The mitigation filters directly reject or decrease the EMF penetrated into the circuit. This idea, however, cannot be applied to existing AIMDs. Moreover, developing EMI filters that are effective over all frequency bands from LF through UHF is not easy.

A warning to dissuade AIMD patients from approaching RFID interrogators too closely is the most practical way of avoiding the EMI risk. Special labels or signs are being affixed to interrogators to indicate that they are EMF sources [19], [20], [43]. However, from the standpoint of absolute risk improvement, it is important to investigate designs that modify the EMF output by the interrogators so as to mitigate the EMI occurrence in AIMD.

According to various studies and experiments on EMI or EMC (Electromagnetic Compatibility), it is well known that the EMI is generally not serious when the interfering EMF has a constant envelope. This is because a constant envelope EMF does not generate low-frequency components in AIMD circuits, which might disturb AIMD operation [25], [28], [29], [39], [40].

This Annex introduces a novel technical possibility of the EMI mitigation method for AIMDs, based on a “mitigation signal”, a ”radio filler” that is superposed between the original EMF flame pulses of the interrogator. This superposition (dummy signal insertion) can be processed at the RFID interrogator using its own transmitter or another circuit. Then, the EMF emitted from RFID interrogator is reshaped from original pulse-modulated to a CW-like signal which causes less EMI on AIMDs than the original EMF. The MID accordingly can be decreased. The MID improvement was experimentally confirmed to be suppressed within 10 cm from the interrogator antenna and vanished at the best case, using some of RFID interrogators of LF, HF and UHF bands commercially available in Japan [36]. Similar results based on the continuous wave RFID experiments are reported by FDA [38]. Therefore, it is generally true that the CW-like signals have a good nature on the AIMD EMI issues. However, since obtained data cannot cover all the 18000 series systems, farther investigations are necessary to conduct on the systems not treated in this technical report. The investigations should involve not only technical but also radio frequency approval (regulation) aspects.

A.2 EMI measurement system

A.2.1 General requirements

The electromagnetic interference (EMI) measurement system is applied to various types of radio frequency identification (RFID) interrogators [1]~[6], [11]~[13] and active implantable medical devices (AIMDs) in practical use and capable of estimating the EMI and the MID characteristics. Accordingly, the system is composed of a saline tank torso simulator (referred to hereafter as a torso phantom) with an AIMD as the device under test, a practical RFID interrogator as the EMF emitter, an interrogator platform if necessary, and electronic measurement instrumentation.

A.2.2 Measurement environment

The measurement is performed in a laboratory conforming to the following environmental conditions:

(1) the effects of EMF from other systems or equipment, reflections, secondary radio frequency (RF) emissions, etc. are small enough so as not to disturb the measurement results;

(2) the ambient temperature is in the range of 18° C to 25° C and the variation of the saline solution temperature does not exceed ±2° C during the test;

(3) compliance with the electromagnetic field (EMF) guidelines concerning human exposure is assured before the RFID interrogator is used in the measurement system [55]~[65].

A.2.3 Measurement system configuration

The measurement system is composed of a torso phantom into which the AIMD can be inserted, a simulated ECG signal generator/AIMD monitor, a chart recorder, an oscilloscope, a measurement platform and the RFID interrogator to be tested. In addition, an appropriate measurement protocol is employed so that precise and reliable EMI assessments are realized in an efficient way.

An example measurement system configuration is presented in Annex A.5.

A.2.3.1 Torso phantom

The torso phantom simulates a standard human chest into which an AIMD is implanted. Its electronic properties are equivalent to those of real humans with respect to simulated ECG signal transmission (low-frequency). Regarding the EMF at high frequency, it is confirmed that conservative measurement results could be obtained even if a saline solution has a low-frequency tissue-equivalent property [31]. Similarly, a flat-shaped torso phantom is preferred over a realistically shaped one because the former yields conservative estimations [15], [23], [31]. A vertical-type phantom is preferable to deal with the weight of gate-type RFID interrogators. Examples of the design parameters of torso phantoms are described in Annex A.6. Differential-detection-type electrodes are used to apply the simulated ECG signals and to monitor the pacing signals through the saline. Details of the electrode configuration are presented in Annex A.7.

A.2.3.2 RFID interrogator platform

An adjustable platform, made of dry wood or polystyrene foam, is used to mount the RFID interrogator and to change its position for determining the MID, as shown in Annex A.5. There is no need to specify the dimensions or size, provided the interrogator EMF is not affected by the platform.

A.2.3.3 Electronic devices

Devices needed are: a simulated ECG signal generator/AIMD monitor, a chart recorder, an oscilloscope and a spectrum analyzer to monitor the interrogator EMF, as well as an AIMD programmer.

A.2.4 EMI evaluation procedure

The EMI evaluation is performed to detect the MID between the RFID interrogator and the phantom surface. The MID is the greatest separation at which the EMI on the AIMD is observed. When a patient who has an AIMD approaches the RFID interrogator closer than the MID at the chest, there is a possibility that the AIMD will perform incorrectly though the patient might not necessarily experience any clinical effect due to it [28],[38].

The detailed processes for observing the EMI and the primary procedure for the MID measurement are described in Annex A.8.

A.2.4.1 RFID interrogator operations

The RFID interrogator should be fixed to a measurement platform and should transmit EMF according to the transmission conditions specified in the relevant operation manual [1]~[6], [11]~[13]. When the output power of the interrogator is adjustable, it should be set at the highest level. The carrier frequency used during the measurements should be set to the centre of the permitted frequency band.

Details are described in Annex A.8.

A.2.4.2 AIMD operations

There are several AIMD manufacturers in the world and many types of AIMDs. Because the MID depends upon the individual AIMD model-type and manufacturer, as well as its operation adjustments, statistically significant numbers of AIMD samples should be obtained.

All features affecting AIMD sensitivity (that are capable of being programmed) should be set to the most susceptible (maximum sensitivity) level. All other parameters should be set to their nominal values; other special functions such as automatic threshold measurement, output control and rate responsive function of the AIMD should be turned off. The AIMD parameters should be printed and recorded on a datasheet.

Detailed of the operation adjustments are described in Annex A.9.

A.2.4.3 Measurement of MID

In each of the various AIMD operation conditions, the MID is determined according to the procedure described in Annex A.8. When no effects are observed, even when the RFID interrogator is almost touching the surface of the phantom, the condition yielding the strongest EMF, the MID is recorded as zero cm or “no effects” and additional processes can be omitted.

A.3 Summary of experiments and evaluation results

Typical examples of RFID interrogators specified by ISO/IEC 18000-2, -3, -4, and -6 have been tested to estimate the EMI and the MIDs of RFID interrogators with various types of AIMDs available in the Japanese market.

From the entire set of measurement results, the characteristics common to all types of RFID interrogators are summarized as follows.

The observed EMI for pacemakers is either a missing pulse(s) or the undesirable generation of asynchronous pulses. The duration of the EMI occurrences vary from a single pulse to the complete inhibition or continuous pulse generation during the RFID interrogator emission. The EMI (including whether or not they occur) depends upon the combination of devices, operation mode, EMI filter performance and various substantial parameters such as the lead length of the AIMD, power, frequency, pulse repetition rate, modulation depth of RFID interrogator, and the distance between the RFID interrogator and the phantom. Examples of the ventricular output pulse time-chart of AIMD EMI are shown in Figures A.1a and A.1b. Figure 1a is a record of pacemaker output during the inhibition test. Here, some intervals between recorded spikes (pacemaker outputs) are prolonged. This means that the pacemaker receives EMI and some of its outputs are inhibited by noise. Figure 1b is a record of pacemaker output during the asynchronous test. The pacemaker is injected with simulated ECG signals with a slightly higher rate than its pacing rate and twice the amplitude as its sensitivity. So the pacemaker outputs would be completely suppressed if EMI did not take place. However, the spikes are seen in Figure A.1b, which mean the pacemaker generated unnecessary outputs due to EMI. These are just a few examples of the impact that the AIMD has on pacemaker output. However, it should be noted that not all the output function effects represent a direct risk to the patient. To elucidate this, clinical and medical discussions are important.

As for ICDs, although this EMI occurs only about 5% of the test cases as shown in A.10.1, when the RFID interrogator antenna and the torso phantom are in close proximity, an inappropriate tachyarrhythmia (fast heart rate) is detected and defibrillation shock is delivered.

Even if different manufacturers' RFID interrogators are constructed to comply with the same standard, MID values may not necessarily be the same. This is because EMI occurrence depends upon the individual RFID interrogator's characteristics such as the spatial distribution of EMF radiated from its antenna, transmission power, frequency, pulse repetition rate, and modulation depth.

Examples of the detailed measurement results are presented in Annex A.10 according to ISO/IEC 18000 series classification.

Notwithstanding the experimental estimations described above, an EMI assessment method based on numerical simulations that can eliminate complicated measurements is proposed in Annex A.11.

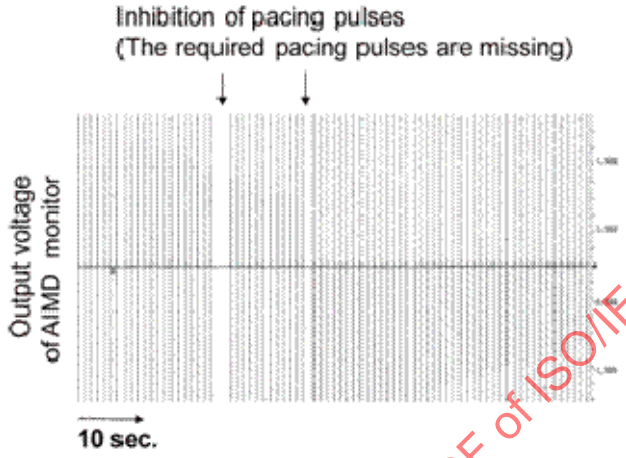

Figure A.1a — Inhibition test result (EMI example)

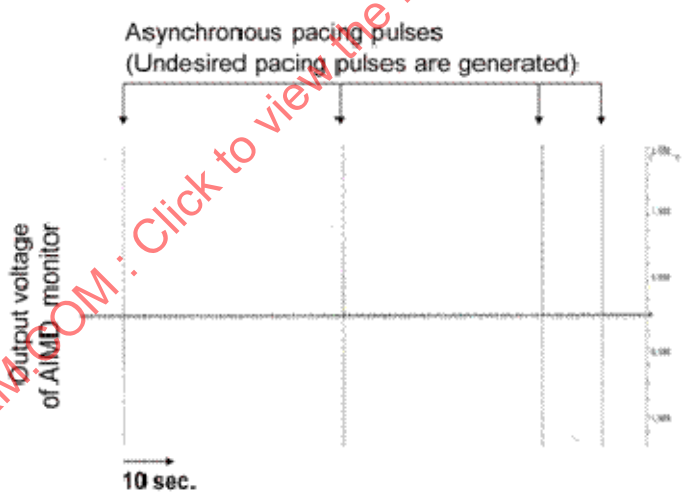

Figure A.1b — Asynchronous test result (EMI example)

A.4 Methods to reduce EMI risk on AIMD due to RFID interrogators

In order to decrease the risk of EMI occurring between ISO/IEC 18000 series RFID interrogators and existing AIMDs, the following methods are proposed.

A.4.1 Warning signage

Safety distance warnings are considered to be effective and are a simple measure to reduce the EMI risk on active implantable medical devices (AIMD) due to various EMF sources, including RFID interrogators. Guidelines for a safety distance of 6 inches (≈15 cm) away from a cellular phone have been adopted in the U.S., EU, and other countries [16], [17]. Similarly, guidelines of 22 cm have been adopted in Japan for cellular phones and lower power RFID interrogators [18]. Also Japan has adopted safety guidelines of 1 m for 4 W EIRP UHF RFID interrogators [20]. Such distances were determined from the MID measurement results and existing safety guideline on the use of cellular phones. In order for AIMD patients to recognize an RFID interrogator and to be made aware of the attendant EMI risk, a label or drawing should be attached to the RFID interrogator. This approach is currently being used in Japan [18], [20], [43]. This measure has been widely adopted for preventing excessive EMF exposure to humans from the various EMF emission sources [55].

A.4.2 Radio filler technique to mitigate EMI influence on AIMD

As is described in the Introduction already, the AIMD EMI trigger due to RFID interrogator EMF is basically attributed to the low frequency noises created by the envelope detection of penetrated EMF at the internal circuit of AIMD. Accordingly, since CW or CW-like signals (i.e. frequency modulation and phase modulation) contains very little low frequency envelope components, so called continuous transmission mode barely causes the AIMD EMI in general. The validity of this hypothesis was experimentally confirmed by a reference [38]. The radio filler technique proposed here uses this mechanism, and in order to transform the original pulse modulated RFID interrogator signal to a CW-like signal, non modulated dummy signals of same or different carrier frequency are fitted into the idle periods between flame signals at the same averaged power level as the RFID interrogator signal. The radio filler technique can decrease the MID with only a small design change to the RFID interrogator that does not impact the basic operation of the system. This improvement is achieved for all types of AIMDs and is applicable for RFID interrogators using frequencies in and above the HF band. The typical experimental data confirmed a reduction of the worst case MID –71 cm for a 4 W EIRP UHF RFID interrogator and a specifically identified AIMD– to just 10 cm [36]. Here, it was inconclusive whether or not the EMI mitigation filter functioned well at the test frequencies in the UHF band for the pacemaker with the worst MID.

Detailed technical information and typical experimental results are described in Annex A.12.

A.5 An example measurement system configuration

The basic configuration of the measurement system and a picture of a practical system are shown in Figures A.2 and A.3, respectively. This basic configuration mirrors those for other RF device tests such as cellular phone handsets [23]~[26], [28], [30], base stations [31] and radio transceivers [15]. In Figure A.2, the simulated ECG signal generator/AIMD monitor supplies the simulated ECG signal to pacemakers and ICDs through the electrodes and lead wires. Pacemakers and ICDs need to sense the simulated ECG signal in order to operate properly. The oscilloscope and chart recorder record the outputs of the pacemaker or ICD. The data recorded allows the occurrence of EMI to be assessed. The distance between the interrogator and the torso phantom front surface can be varied during the test; the MID is measured in units of centimetres.

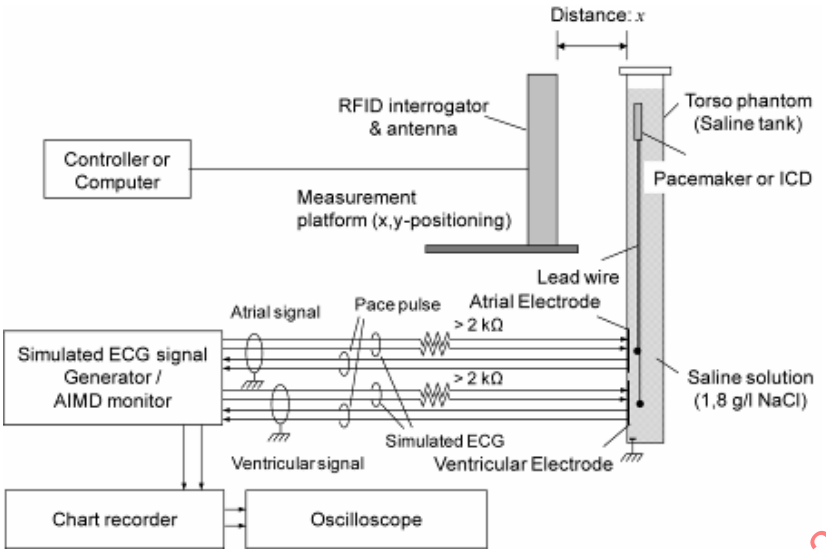

Figure A.2 — Basic configuration of EMI measurement system

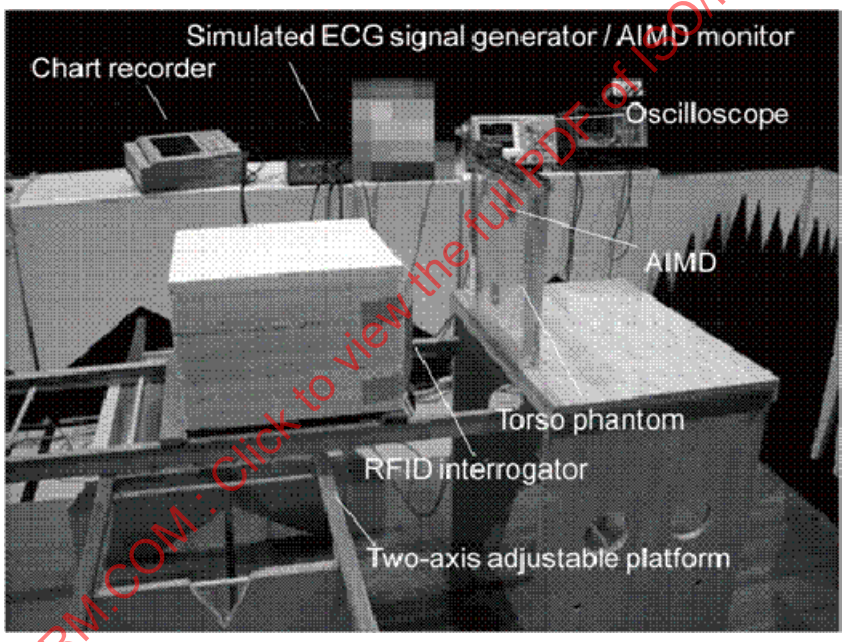

Figure A.3 — Overview of measurement system

A.6 Torso phantoms

A.6.1 Fundamental construction

To measure the EMI on an AIMD from an RFID interrogator, a human torso phantom can be constructed based upon designs that have been widely used in cellular phone EMI studies. Since gate-type RFID interrogators are installed upright and humans will walk past or stand next to the RFID interrogator, a vertical-type torso phantom is preferred, including a realistic human-shaped one [39]. Moreover, it is easier to change the distance between the RFID interrogator and the torso phantom using a vertical phantom than it is to change the distance using the horizontal phantom specified in ANSI/AAMI PC69.

An example of vertical torso phantom is shown in Figures A.4 and A.5. The size of the phantom is almost the same as that first proposed by Irnich [15], [21].

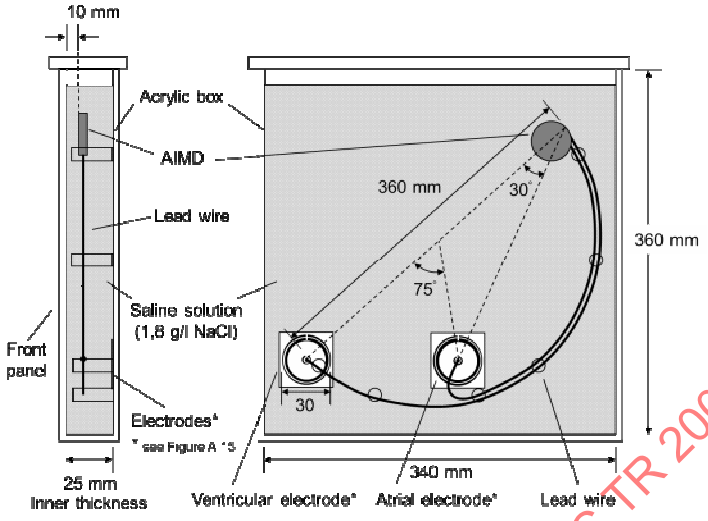

Figure A.4a — Side view **Figure A.4b — Front view**

Figure A.4 — Example of vertical torso phantom

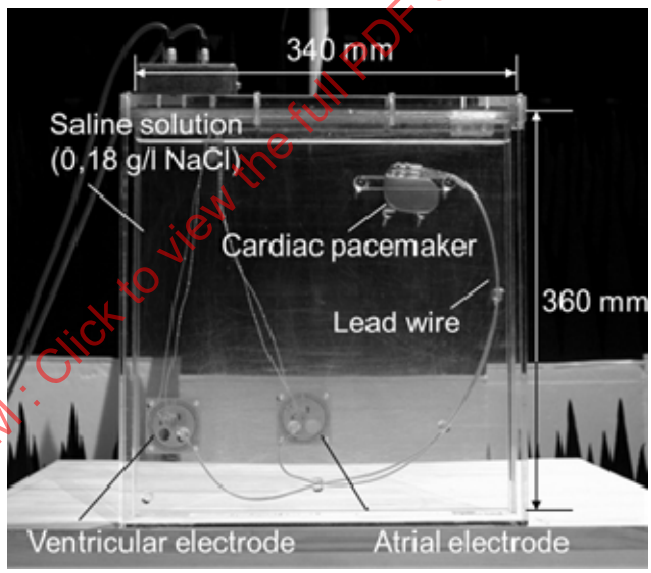

Figure A.5 — Vertical torso phantom

Table A.1 — Relative dielectric constant and conductivity for saline solution, skin, lung and muscle

	Relative dielectric constant					Conductivity [S/m]				
Frequency [MHz]	0,125	13,56	433	915	2 450	0,125	13,56	433	915	2 450
1,8 g/l NaCl* [1]	77	77	77	77	75	0,23	0,23	0,29	0,50	1,51
Skin (wet) * [2]	14000	180	49	46	43	0,07	0,38	0,68	0,85	1,59
Lung (Deflated) * [2]	4400	150	54	51	48	0,28	0,45	0,69	0,86	1,68
Muscle (Parallel Fiber) * [2]	8500	1300	59	57	54	0,40	0,68	0,85	1,00	1,88

*1: Data of 433~2 450 MHz were measured using a coaxial probe method [48], and those of 0,125 and 13,56 MHz were extrapolated with a Debye equation [49].

*2: Data are from [50].

A.6.2 Saline solution

The torso phantom is comprised of a saline tank and electrodes, as shown in Figure A.4. The saline tank is constructed from acrylic panels and is filled with a saline solution, with the density (1,8 g/l NaCl concentration) specified in ANSI/AAMI PC69 and [26]. For radio frequencies from 433 MHz to 2,45 GHz, the saline conductivity ranges from 0,29 to 1,5 S/m, while the saline relative dielectric constant is approximately 75~77. The conductivity and the relative dielectric constant of an actual human torso are reported to be approximately 0,69~1,7 S/m and 50, respectively [50]. The electric field strength inside the torso phantom at 900 MHz was calculated using the FDTD method to estimate the difference in the dielectric characteristics between the saline solution and actual human tissue. As a result, the electrical field strength at the saline solution surface where the AIMD was implanted was found to be equal to or 2 dB higher than that of an actual human tissue model. This means that the AIMD EMI measurement system that uses the proposed torso phantom provides conservative figures [31].

Relative dielectric constants and conductivities for saline solution, skin, lung and muscle are listed in Table A.1. At 125 kHz and 13,56 MHz, as EMI is mainly caused through magnetic field coupling, the differences of the relative dielectric constants between saline solution and actual human torso could be ignored.

The positions of the AIMD and the lead wires are fixed by using acrylic stays. The acrylic material used has a dielectric constant and loss tangent of approximately 2~5 and below 0,004 in the frequency range of 125 kHz to 2,45 GHz, respectively.

A.6.3 Acrylic panel

As the saline tank should be sturdy and not distort under the weight of the saline solution, the acrylic front panel must be sufficiently thick while not so thick that the EMI assessments are affected. Thus, the front panel was constructed with 5 mm thickness.

In order to estimate the impact of the acrylic plate, numeric simulations based upon FDTD method [54] were conducted. The analysis model and its coordinate system are shown in Figures A.6 and A.7, respectively. Although plane wave irradiation is assumed, a 3-dimensional phantom model with the same size as that

shown in Figure A.4 was analyzed. An example of electric field distributions obtained at 950 MHz is shown in Figure A.8. In this Figure, two electric fields inside the saline solution, for the cases of with and without the acrylic front panel, are calculated and plotted by solid and dotted lines, respectively. A comparison of the fields shows that the differences between them are within ±0,1 dB and hence the acrylic front panel effects are negligible. At frequencies between 125 kHz and 2,45 GHz, relative dielectric constant and conductivity of the acrylic panel are about 2-5 and less than 0,004 S/m, respectively. As these values are far less than those of the saline solution and due to relative thinness of the acrylic panel, its effect on the EMF from LF and HF RFID interrogators can be neglected as is true for the UHF case.

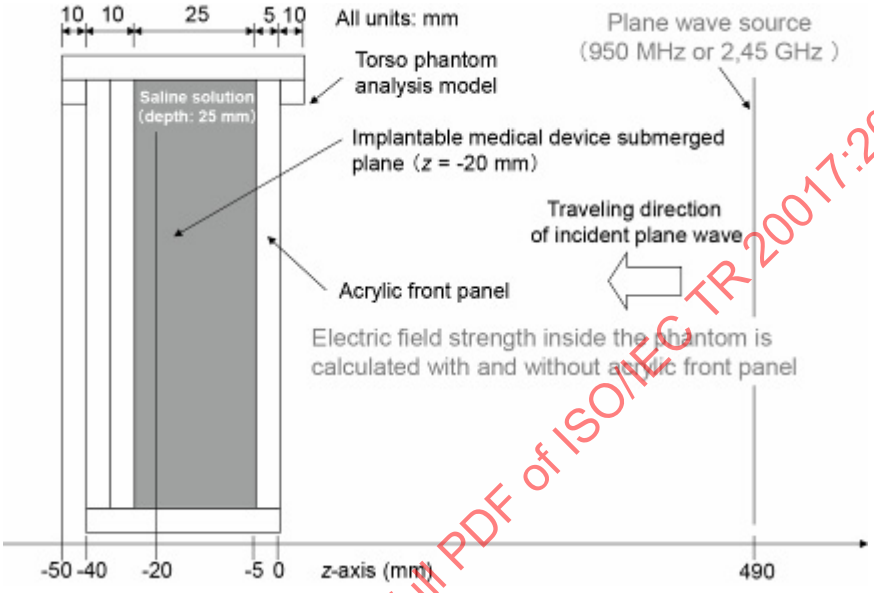

Figure A.6 — Analysis model for torso phantom

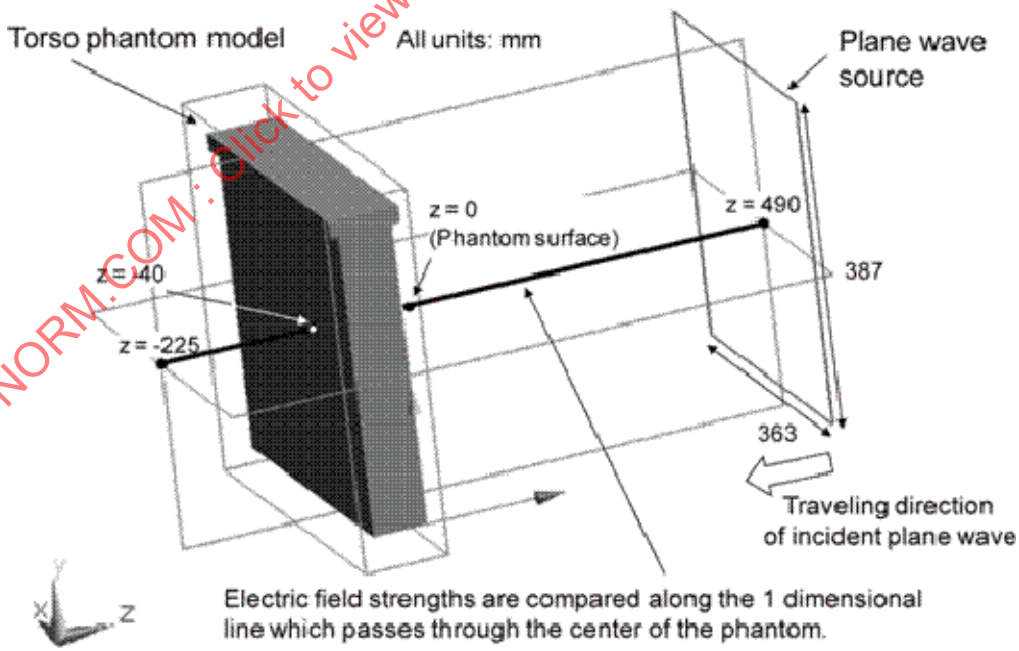

Figure A.7 — Coordinate system for analysis model

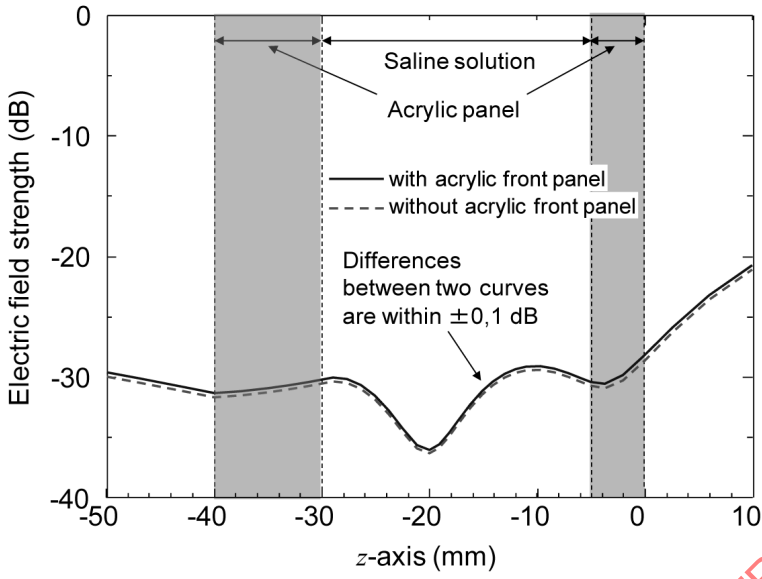

Figure A.8 — Electric field distributions inside of phantom (950 MHz)

A.6.4 Thickness of the saline solution

With respect to the inner thickness of the saline tank shown in Figure A.4, the 25 mm of the experimental system is about 1/5th that specified by ANSI/AAMI PC69, which is about 150 mm. This reduction is necessary to decrease the phantom weight. Since magnetic interaction dominates the EMI at frequencies below several tens of MHz, the thickness of the saline solution does not alter the EMI estimation results. At higher frequencies, however, this reduction might excite an undesirable standing wave (internal EMF) in the saline solution. Figure A.9 shows the analysis model for the thickness simulation using the FDTD method. Figures A.10 and A.11 show the analysis results of electric field penetration for 25 mm and 150 mm saline solution thicknesses, respectively. Incident waves are 433 MHz, 950 MHz and 2,45 GHz continuous plane waves from the outside in the z-axis direction. This is because the standing wave in the depth direction is most strongly created when the incident plane wave is perpendicular to the front of the torso phantom (including near field irradiation cases). Results show that standing waves are created inside the saline solutions regardless of thickness. The electric field levels of one-dimensional standing waves created along the z-axis near the AIMD are plotted in Figures A.10 and A.11 in which dash-dotted, solid and dotted lines indicate 433 MHz, 950 MHz and 2,45 GHz characteristics, respectively. The AIMD standard location is drawn in these Figures, and it is estimated that even if the AIMD position is moved a few mm, the electric field created around the AIMD is likely to remain constant within 3 dB at 950 MHz and 2,45 GHz. Accordingly, the Irnich type phantom can be used in UHF and 2,45 GHz bands, provided this level of uncertainty is acceptable. However, in order to avoid the creation of a deep electric field dip of about 10 dB at 433 MHz, it is necessary to use a 150 mm thick tank.

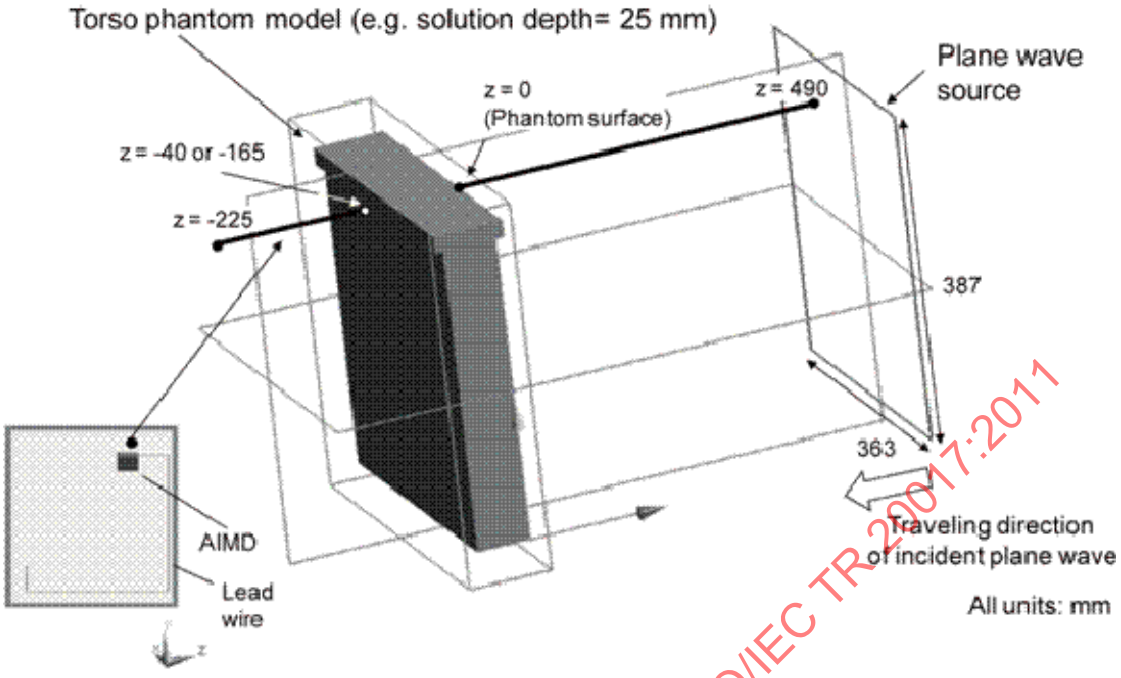

Figure A.9 — Analysis model for thickness simulations

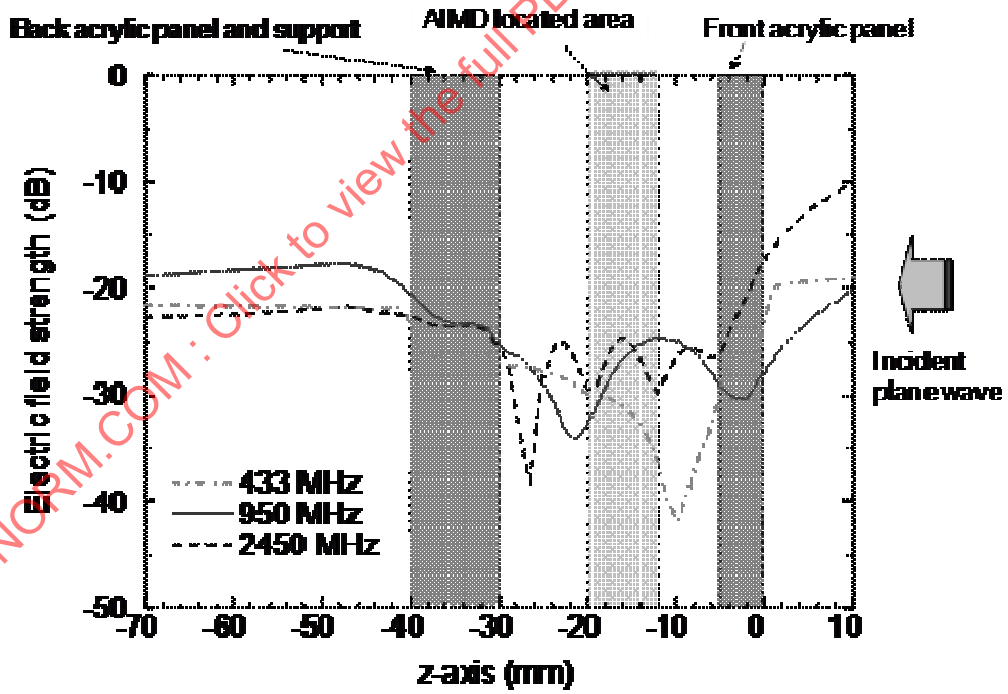

Figure A.10 — Electric fields for 25 mm thickness

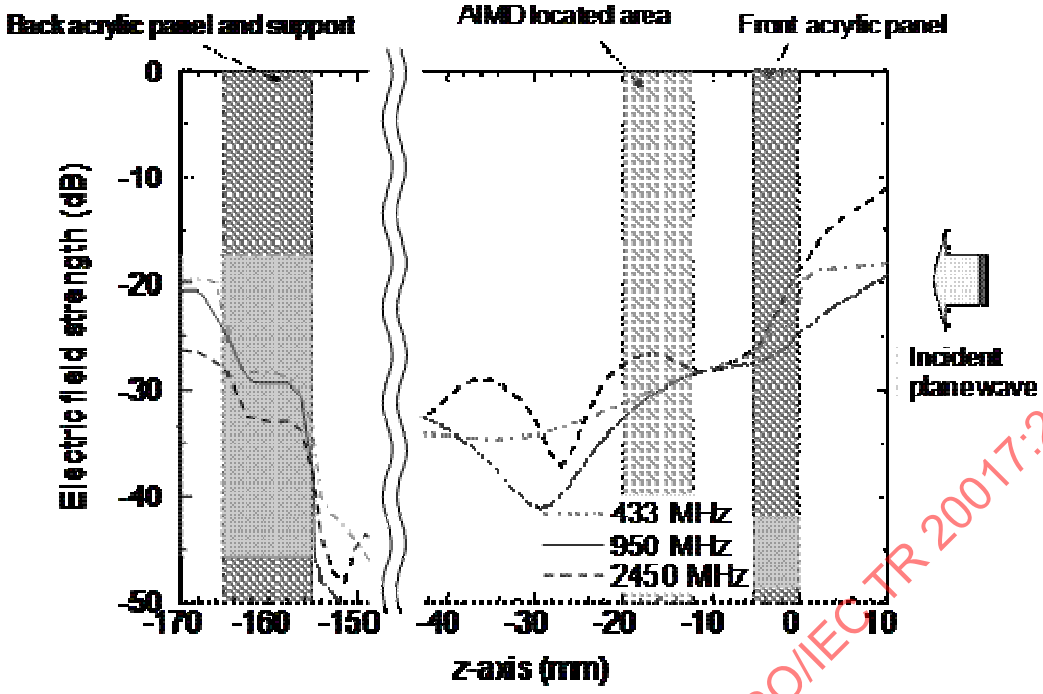

Figure A.11 — Electric fields for 150 mm thickness

A.6.5 Standing wave suppression

When more reliable and more repeatable estimations are required, it is important to suppress the standing waves inside the saline solution as much as possible. For this reason, a phantom structure with an EMF-absorbing plate attached to the back of the cavity was developed, see Figure A.12. The dielectric plate is made from a newly developed silicon rubber material [55] whose relative dielectric constant 50 and conductivity 2,0 S/m at 950 MHz are determined by parameter searching computation so as to suppress the standing wave most effectively in the UHF band. Examples of the simulation and experimental results shown in Figure A.13 confirm that standing waves are effectively suppressed in the 25 mm configuration (Figure A.10) to the same levels as seen in the 150 mm configuration (Figure A.11), so an easy handling vertical phantom can be realized. Electric field strengths are compared along the one-dimensional line located at the centre of the phantom as shown in Figure A.7. In addition, with respect to magnetic field penetration into the phantom, since the silicon rubber material has a relative permeability of one, the new phantom has the same properties as the Irnich type phantom in the LF and HF bands, and thus supports those frequencies as well as UHF.

Figure A.14 shows an example of the 3D electric field distributions predicted by the FDTD analysis around the AIMD for the 950 MHz case. From this figure, the estimations in A.6.4 and A.6.5 at one position remain valid for some distance, within a tolerance of 3-5 dB, over the AIMD front area.

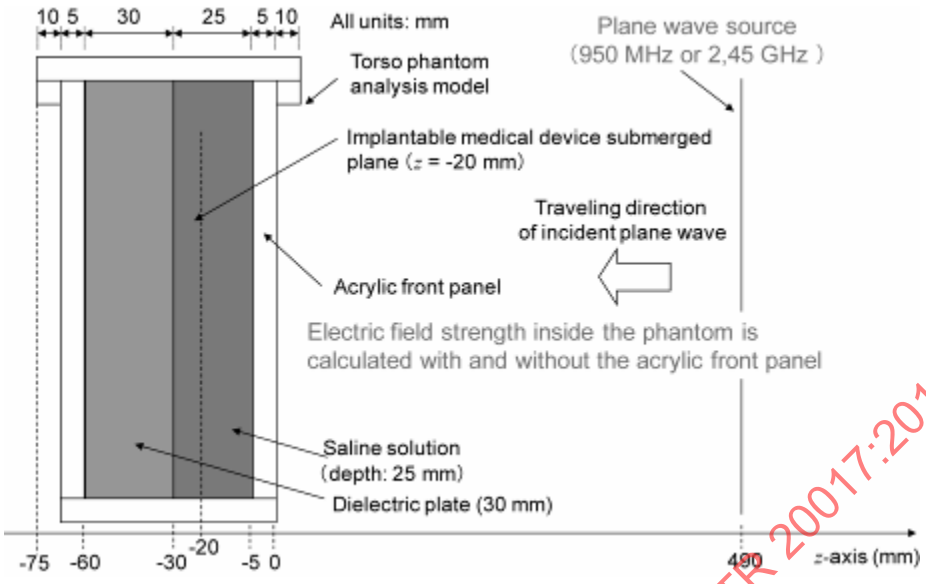

Figure A.12 — New phantom with absorbing back plate

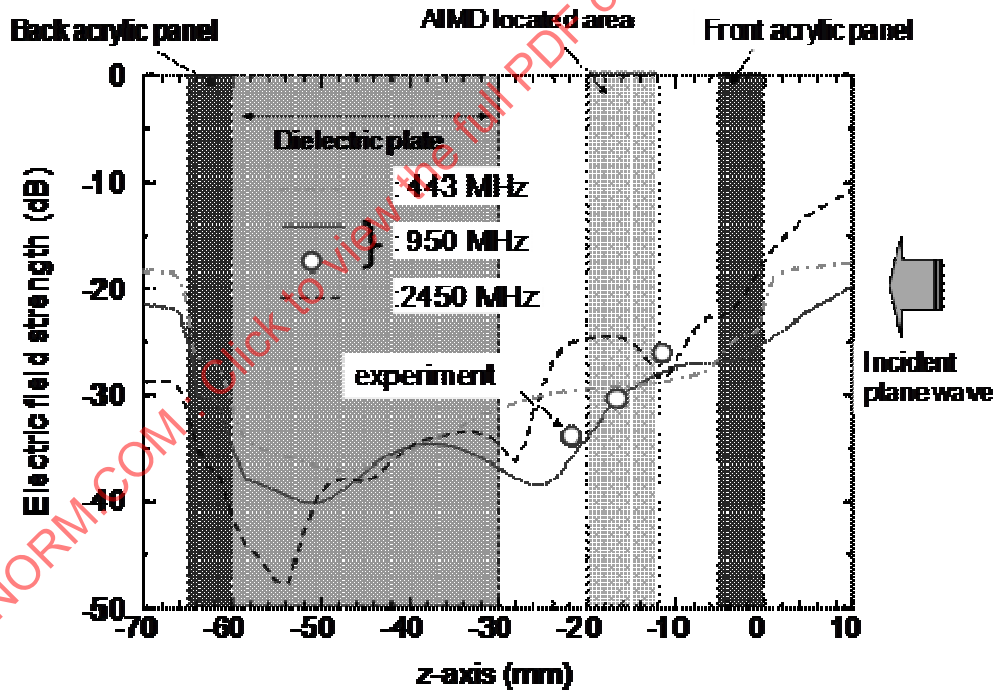

Figure A.13 — Standing waves inside the new phantom

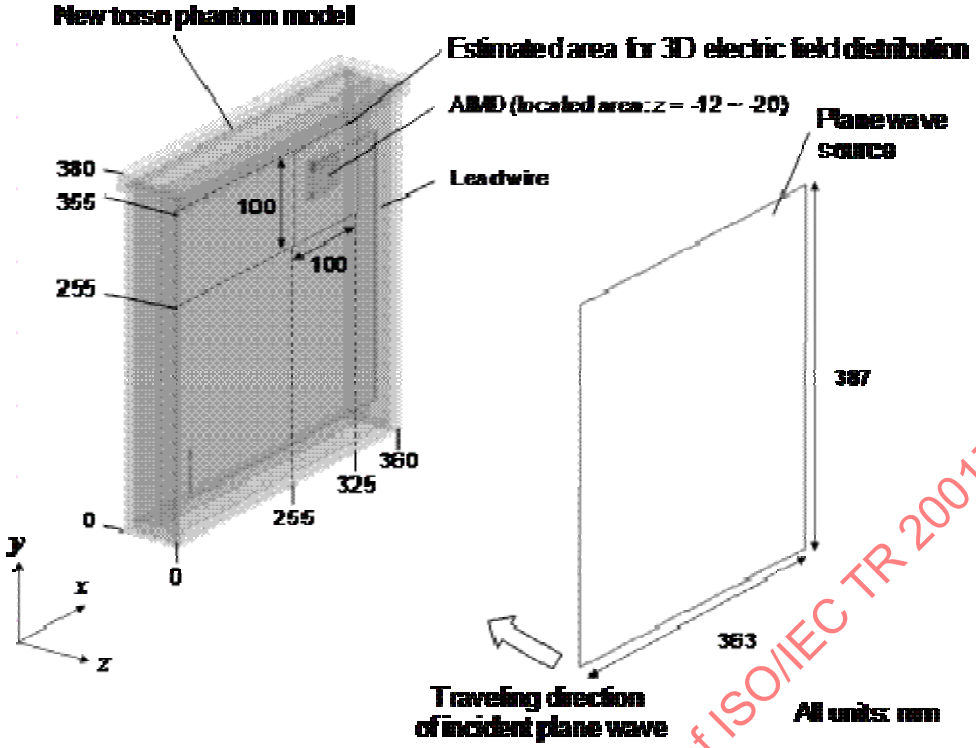

Figure A.14a —Analysis model for 3D EMF distribution simulation

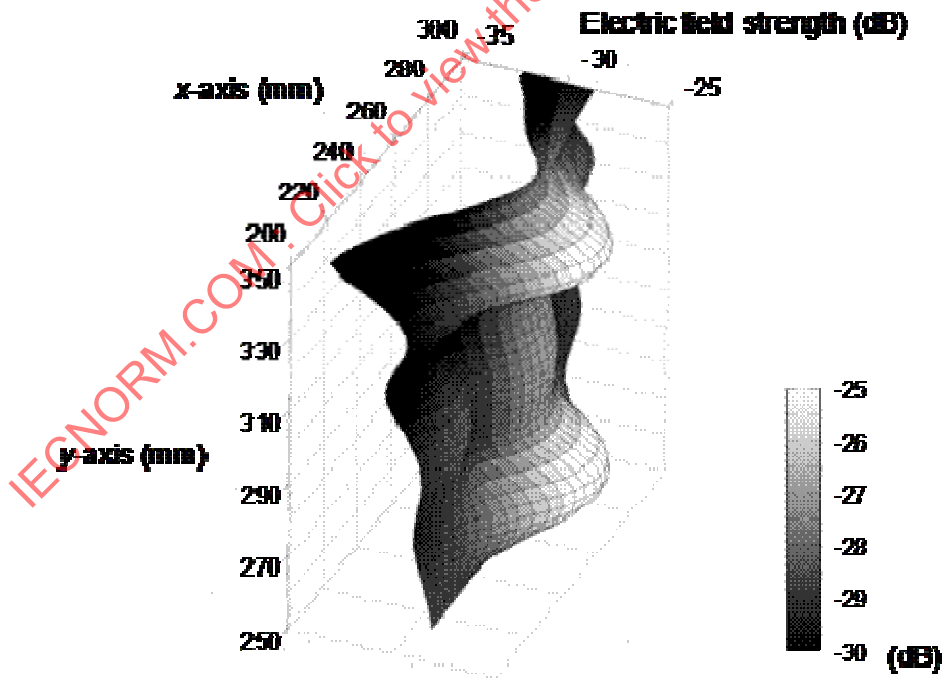

Figure A.14b —3D electric field distributions around the AIMD for 950 MHz

Figure A.14 —A typical example of 3D EMF distributions around the AIMD

A.7 Electrode to control/monitor AIMD

As shown in Figure A.4, the electrodes are installed inside the saline tank as dual-chamber pacemakers equipped with atrium and ventricle lead wires, or single-chamber pacemakers. An example of the interface circuit construction between the electrodes and the external electronic devices is shown in Figure A.15. Fundamental specifications are similar to those described in ANSI/AAMI PC69 and [41]. The electrodes are constructed from coaxial stainless steel rings and a small patch, as shown in Figure A.15. The electrodes are positioned near the end of the lead wire, but without directly contacting the AIMD lead wires. Thus, all types of lead wires can be easily installed inside the phantom without modification. Signal flow for the inhibition test: The pace pulses generated by the pacemaker are received at each electrode. These pulses are then input to the differential amplifier shown in Figure A.15. This construction detects only the differential voltage between the outer ring and the centre patch. While the leakage signal from the another end of the lead wire impresses almost the same voltage on these ring and patch, therefore two electrodes for atrium and ventricle can be electrically highly isolated each other. And thus the dual chamber test in one saline tank is realized with high separation performance between two chamber output signals. Signal flow for the asynchronous test: The signals from the ECG generator are fed to the differential driving circuit shown in Figure A.15. These signals are then applied to each electrode. The ECG signals that leak into the monitor circuit can be cancelled by the bypass ECG signals through the amplitude/phase adjuster circuit shown in Figure A.15. By using this coaxial electrode configuration, separation of the simulated ECG signals between the atrium and ventricle lead wires can be maintained at a level greater than 20dB, which enables high sensitivity EMI tests to be conducted on dual chamber pacemakers [31]. In addition, the double ring construction allows high immunity against external electromagnetic disturbances to be achieved by adopting the differential detection.

In order to estimate the resonance characteristics of the electrode, S11 (reflection performance) of the electrode was measured as shown in Figure A.16. No serious resonances are observed in the RFID frequency bands. This means that the electrode did not pick up any RFID signals selectively. Here, at UHF frequencies, since the line impedance between electrode and monitor circuit is not matched to transmit UHF signals, the resonance observed in the UHF bands could not affect the monitoring circuit.

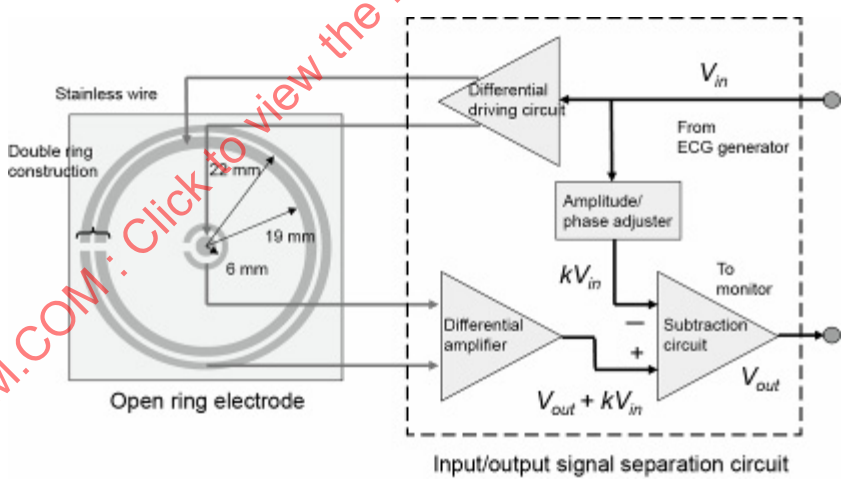

Figure A.15 — Electrode and interface circuit

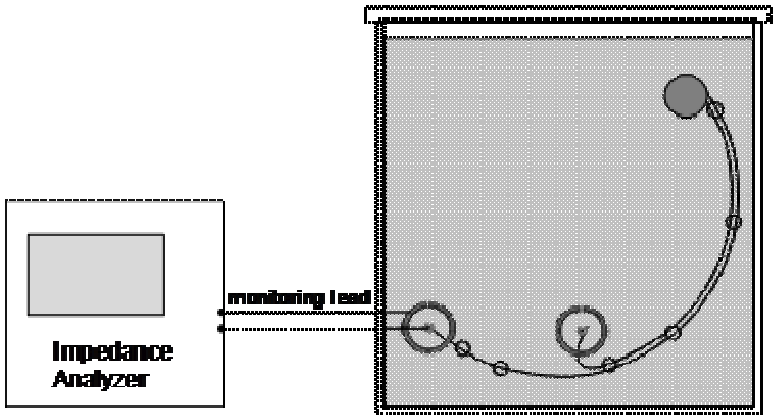

Figure A.16a — measurement setup

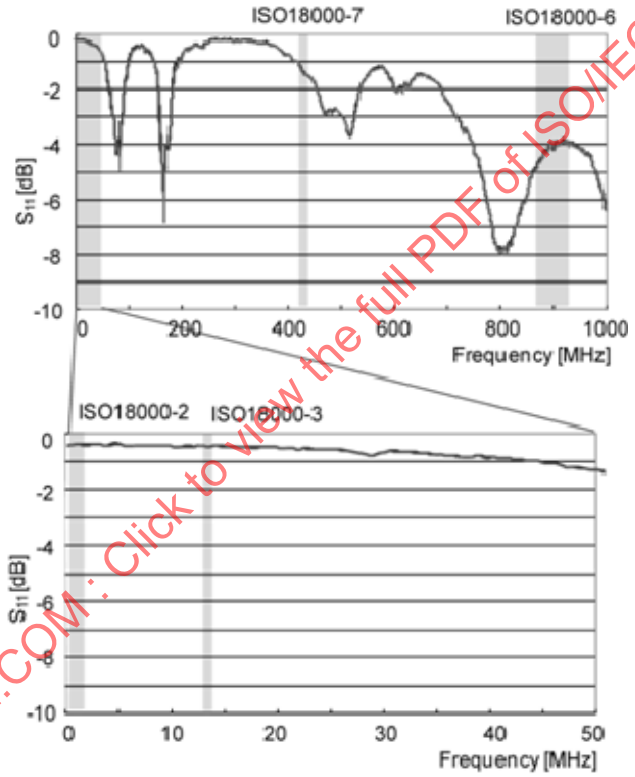

Figure A.16b —S11 frequency responses

Figure A.16 — Measurement for the S_{11} frequency responses of the electrode

A.8 Measurement procedure

EMI experiments consist of an “inhibition test” and an “asynchronous test”. In this report, an EMI is recorded as having occurred if any change in the pacing behaviour of the pacemaker or any inappropriate delivery of tachycardia therapy of ICD is observed during one measurement step of 100 seconds. This determination criterion is based upon an engineering standpoint, and clinical significance estimations remain to be discussed [22], [32].

- An inhibition test examines the omission of pacing pulses by AIMDs. There is no injection of the simulated ECG signal during the inhibition test. An example of an inhibition test result is shown in Figure A.1a. The required pacing pulse is inhibited due to EMI.

- The asynchronous test examines the generation of fixed rate asynchronous pulses. A simulated pulse is injected during the asynchronous test. An example of an asynchronous test result is shown in Figure A.1b. When there is no EMI, the AIMDs sense the simulated pulse and the pacing pulse is inhibited. However, an asynchronous pulse is generated when the AIMDs appropriately recognize noise and switch to noise reversion mode. In addition, inappropriate tachyarrhythmia (fast heart rate) detection and delivery of therapy/shock were also investigated in the EMI experiments on ICDs.

As shown in Figure A.17, the procedure of the EMI experiments differed slightly depending on the antenna type. The common points for all antennas are as follows:

1) First of all, program the sensitivity, on both pacemakers and ICDs, to the maximum level and the refractory period to the shortest time. This setting gives the most conservative results.

2) Record the simulated ECG signal for each mode on paper for 100 seconds. The distance between the antennas and the torso phantom is increased when interference occurs. In this case, the MID (distance at which EMI disappears) is determined and recorded in centimetres.

3) Lower the sensitivity of pacemakers and ICDs in five steps (maximum, approximately 1,0 mV, approximately 2,4 mV, approximately 5,6 mV, and minimum) and record the MID, if found.

4) Record the measurements for all combinations of antennas and AIMDs. The operating modes of pacemakers and ICDs include unipolar and bipolar mode and VVI and AAI mode.

The differences due to the types of antenna are as follows:

Process 1 for handheld and stationary antennas: The human torso model is placed parallel to the antenna. The antenna is then moved from side to side, y-axis in Figure A.18, while making the measurements. The MID is the distance between surface of the antenna and the human torso model.

Process 1 for the gate-type antenna: The human torso model is located on the perpendicular bisector of the line between the two gate antennas, see Figure A.19. Distance D is then changed to determine the MID. Distance D is taken as the spacing between the centre of the antenna (width direction) and the centre of the human torso model (depth direction).

If distance D in process 1 reaches 0 cm, move to process 2.

Process 2 for the gate-type antenna: The human torso model is located on the centre of the line between the two gate antennas, as shown in Figure A.20. In addition, the model is also located at the centre of the antenna (width direction). Distance L is then changed to determine the MID. At each L value, the angle of the human body model is changed by plus/minus 45 degrees. Distance L is the spacing between the antenna surface and the centre of human torso model (depth direction).

If distance L in process 2 reaches 20 cm, move to process 3.

Process 3 for the gate-type antenna: The human torso model is located on the centre of the antenna (width direction), as shown in Figure A.21. Distance L is then changed to determine the MID. Distance L is defined as in process 2.

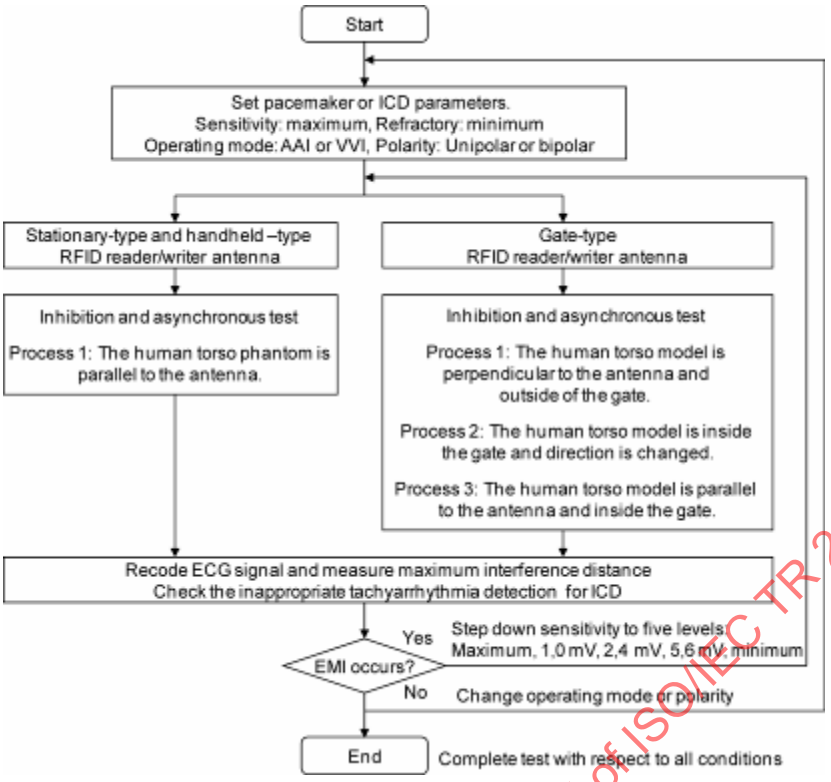

Figure A.17 — Fundamental measurement procedure

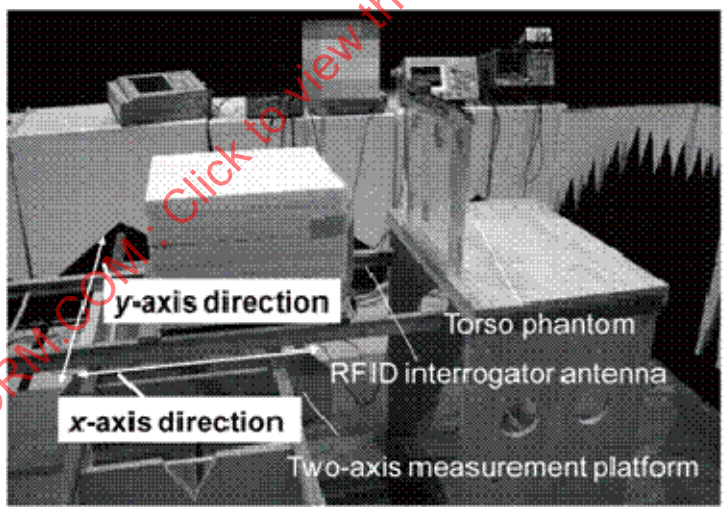

Figure A.18 — Measurement system (handheld- and stationary-type)

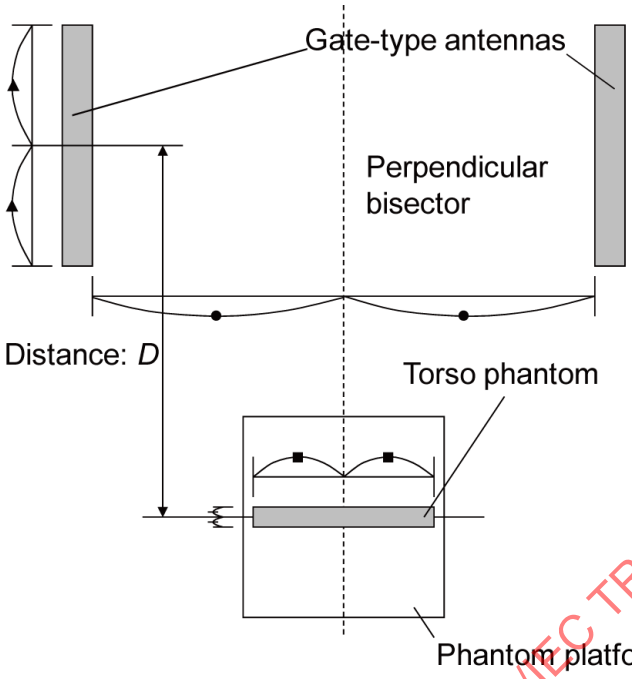

Figure A.19 — Test process 1 for the gate-type antenna

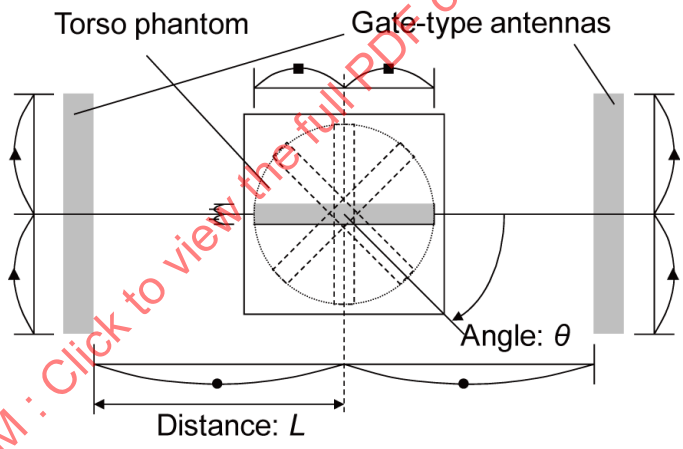

Figure A.20 — Test process 2 for the gate-type antenna

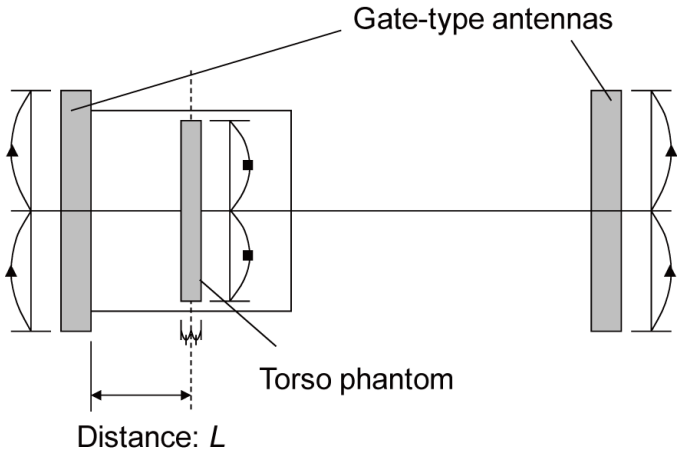

Figure A.21 — Test process 3 for the gate-type antenna

A.9 Operation conditions of AIMD

The initial settings of the AIMDs for the EMI experiments are shown in Table A.2. To obtain conservative EMI estimation results, the AIMD is set to its highest sensitivity and shortest refractory period. In addition, its pacing rate is set to 60 ppm (pulses per minute). The experiments are conducted in both pacing modes of AAI (the Atrium chamber is paced; the Atrium chamber is sensed; and the response to sensing is Inhibited) and VVI (the Ventricle chamber is paced; the Ventricle chamber is sensed; and the response to sensing is Inhibited) for single chamber AIMDs. In case that the device under test is a dual chamber type, it should be tested in two single chamber modes, i.e.: the atrial chamber and ventricular chamber separately, to make the judgement of EMI occurrence easier. Also the experiments should be conducted with sensing and pacing polarities of both bipolar and unipolar. To sense the ECG signal and pace the heart, an AIMD uses two electrodes - a different electrode and an indifferent electrode. And most of the AIMDs have two operating modes depending on the configuration of the electrodes. One mode is called "unipolar". In this mode, the AIMD uses its metal housing as the indifferent electrode and the tip electrode at the end of the lead wire as the different electrode. The other is called "bipolar". In this mode, the difference electrode is the tip electrode and the indifferent electrode is a ring electrode, which is located about 1 cm away from the end of a lead wire.

Details are obtained from references [42] and references in AAMI TIR18.

Table A.2 — Initial settings of pacemaker

Parameter	Value
Stimulation mode	AAI or VVI
Heart rate	60 ppm
Pacing and sensing polarity	Unipolar or bipolar
Pulse amplitude and duration	Nominal values (Approximately 3,5 V and 0,4 ms)
Sensitivity	Maximum (most sensitive)
Refectory period	Minimum

A.10 Measurement results of RFID interrogator examples

A total of 27 AIMDs were examined, and their major functions and approval year are listed in Table A.3. The lead wire lengths for ventricular, atrial and ICD were 58-59 cm, 52 cm and 59-65 cm respectively. Either a bipolar or unipolar lead was used depending on the AIMD. Since it took about two years to complete all tests and it was difficult to keep all of the same AIMDs during the whole test period, the number of AIMDs in each test changed. In addition, since they had different operation modes, a total of 720 measurements were conducted. The EMI occurrence rate *P* of the vertical axis is defined as $P = M_{affected} / M_{total} \times 100$ (%).

Where, $M_{affected}$ is observed as the number of affected modes at each test distance (see Annex A.8), and M_{total} is the total test mode number at each sensitivity level of the AIMDs.

Table A.3 — AIMDs used for test groups ISO 18000-2/-3/-4/-6

AIMD				Test groups			
Type	Chamber	Polarity	Approval year*	ISO 18000-2 (Type A)	ISO 18000-3 (Mode 1)	ISO 18000-4 (Mode 1)	ISO 18000-6 (Type C)
Pacemaker	Single	Program-mable**	- 1999	7	7	6	2
			2000 - 2004	3	3	3	1
			2005 -	0	0	0	0
		Bipolar	- 1999	0	0	0	0
			2000 - 2004	1	1	1	0
			2005 -	0	0	0	0
	Dual	Program-mable**	- 1999	1	1	1	2
			2000 - 2004	7	7	7	7
			2005 -	1	1	1	13
ICD	Single	Bipolar	- 1999	0	0	0	0
			2000 - 2004	0	0	0	0
			2005 -	2	2	3	0
	Dual	Bipolar	- 1999	0	0	0	0
			2000 - 2004	2	2	2	1
			2005 -	3	3	3	11

*: Approval year in Japan
**: Selectable either unipolar or bipolar polarity mode

A.10.1 ISO/IEC 18000-2, Type A

Four different types of RFID interrogators under the continuous transmission mode, as basically specified by ISO/IEC 18000-2 Type A were tested [2]; their technical details are listed in Table A.4. The results from the inhibition and asynchronous tests at different pacemaker sensitivities are shown in Figure A.22.

At the highest sensitivity and the distance of within 4 cm, the total affected mode number and *P* were 161 and 29,3%, respectively.

With regard to the pacemaker function of implantable cardioverter defibrillators (ICDs), the results from the inhibition and asynchronous tests at different sensitivities are shown in Figure A.23.

At the highest sensitivity and the distance of within 4 cm, the total affected mode number and *P* were 27 and 30,7%, respectively.

With regard to the defibrillator function of ICDs, the results from the false positive and false negative tests at different sensitivities are shown in Figure A.24. The false positive test is finding tachyarrhythmia detection of ICD when the patient does not have ventricular tachycardia. The false negative test is to inhibit tachyarrhythmia detection of ICD when the patient has actually ventricular tachycardia.

In the false negative test, the ICD is injected with an ECG signal that simulates ventricular fibrillation (240 bpm) via the ventricular electrode. In addition, the therapy function of ICD is stopped if possible.

At the highest sensitivity and the distance of within 4 cm, the total affected mode number and *P* were 6 and 7,3%, respectively.

The worst MIDs in the inhibition test were 16 cm for pacemakers and 15 cm for ICDs. In the asynchronous test, they were 17 cm for a pacemaker and 4 cm for an ICD.

For low-band RFID interrogators using 125 kHz and HF (13,56 MHz), inductive coupling is used to allow communication between RFID interrogator antenna and tags. Accordingly, the magnetic field from the RFID interrogator antenna might impose significant EMI on the AIMDs.

With regard to this supposition, experimental studies were conducted and it was confirmed that EMI occurrence depends on the total magnetic flux that is interlinked with the one turn coil formed with the AIMD, the lead-wire and the direct body current path in the torso phantom [33], [35].

Contrary to the above results, other MIDs were measured using the same kind of experiments listed in report [38]. It is assumed that the MID differences can be chiefly attributed to the pulse repetition rate of RFID interrogators used in the experiments. In report [38], pulse repetitions were set from 4 Hz to 25,8 Hz, while in this TR the default setting was continuous transmission (no repetition), which lessens the EMI on AIMD to a greater extent than low frequency pulsed transmission.

Table A.4 — RFID interrogators tested (ISO/IEC 18000-2, Type A)

Frequency	Less than 135 kHz
Transmission method	Magnetic coupling
Maximum communication distance guaranteed	~50 cm
Modulation	Amplitude shift keying (100%)
Air interface protocol	Type A
Bit rate	Average 5,2 kbit/s
Transmission mode	Continuous
Application type	Stationary
Number of devices	4
Antenna size	15 × 12 × 5,7 cm^3, 20 × 20 × 3,5 cm^3, 65 × 20 × 3,5 cm^3, 72 × 50 × 16 cm^3

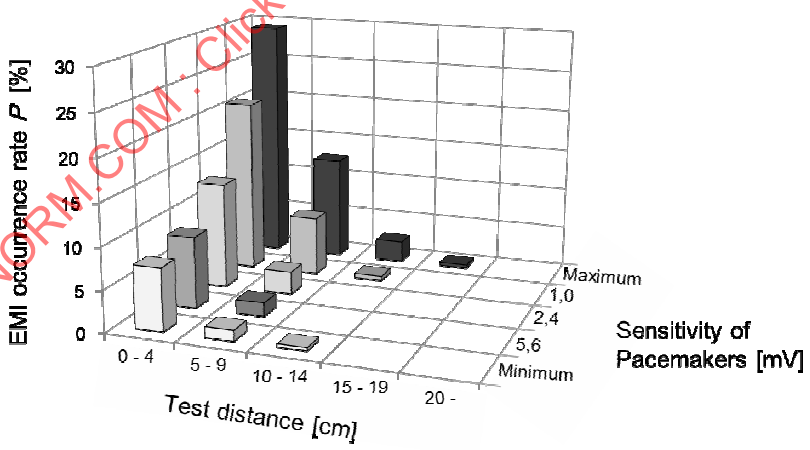

Figure A.22 — Test results of ISO/IEC 18000-2, Type A RFID interrogators and pacemakers (Inhibition and asynchronous tests at different sensitivities)

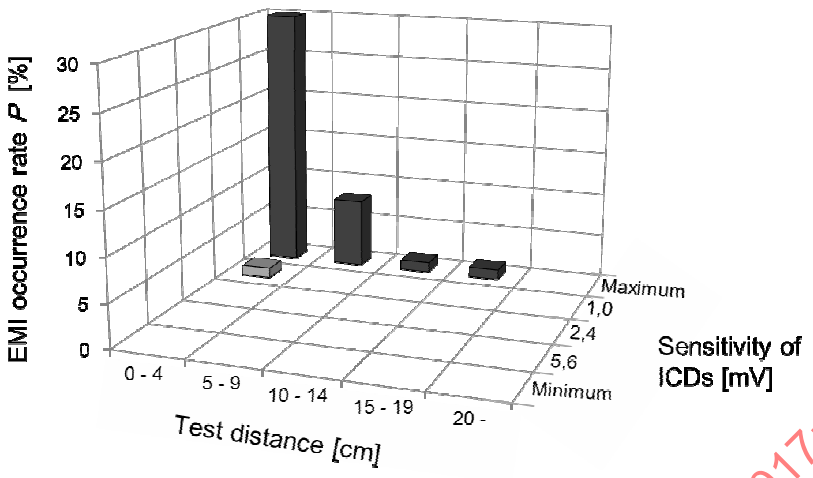

Figure A.23 — Test results of ISO/IEC 18000-2, Type A RFID interrogators and ICDs (Inhibition and asynchronous tests at different sensitivities)

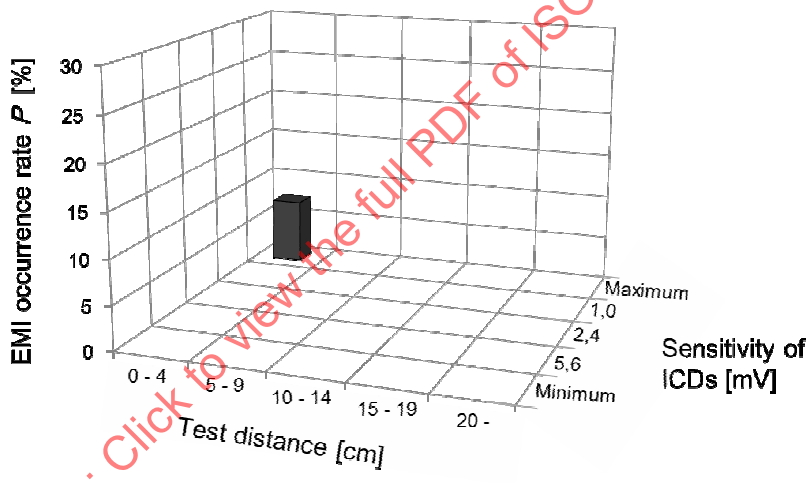

Figure A.24 — Test results of ISO/IEC 18000-2, Type A RFID interrogators and ICDs (False positive and false negative tests at different sensitivities)

A.10.2 ISO/IEC 18000-3, Mode 1

26 different types of RFID interrogators of the Mode 1 specified by ISO/IEC 18000-3 [3] were tested; their technical details are listed in Table A.5. The same AIMDs were used as those subjected to the ISO/IEC 18000-2 tests (see Table A.4). The total number of measurements were 1 021 for the handheld-, 814 for the stationary-, and 438 for the gate-type RFID interrogators.

Table A.5 — RFID interrogators tested (ISO/IEC 18000-3, Mode 1)

Frequency	13,56 MHz		
Transmission method	Magnetic coupling		
Maximum communication distance guaranteed	~60 cm		
Modulation	Amplitude shift keying (100% and 10%)		
Air interface protocol	Mode 1		
Bit rate	26,48 kbit/s, 1,65 kbit/s		
Application type	Handheld	Stationary	Gate
Number of devices (Transmission mode)	9 (Continuous) 4 (Intermittent)	12 (Continuous)	2 (Intermittent)
RF usage of Intermittent wave (Pulse period, Pulse width)	(250 ms, 50 ms), (350 ms, 230 ms), (350 ms, 210 ms), (250 ms, 145 ms)		(300 ms, 100 ms), (20 ms, 10 ms)
Antenna size	All are about 7,5 × 16 × 4 cm^3	All are about 30 × 30 × 4cm^3	170 × 32 × 29 cm^3, 165 × 75 × 12 cm^3

A.10.2.1 Handheld-type antenna

For the handheld-type antennas, the results gathered from the inhibition and the asynchronous modes are shown in Figure A.25. No EMI was observed for any ICD.

At the highest sensitivity, the total affected mode number and *P* were 8 and 0,9%, respectively. The worst MID is 3 cm for a pacemaker.

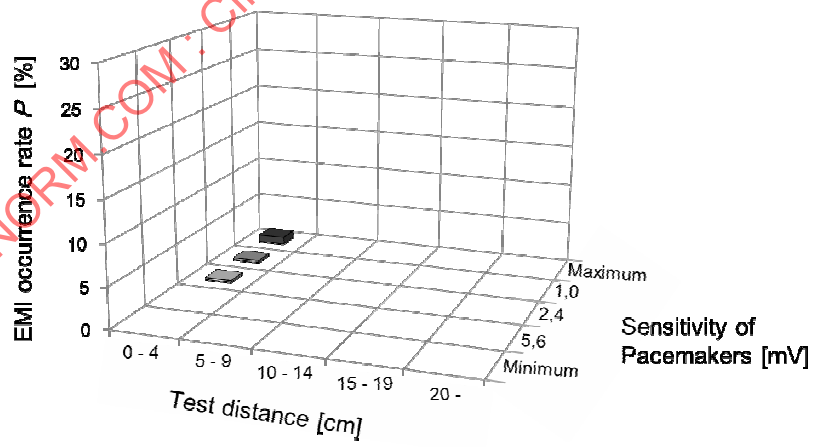

Figure A.25 — Test results of ISO/IEC 18000-3, Mode 1 handheld type RFID interrogators and pacemakers (Inhibition and asynchronous tests at different sensitivities)

A.10.2.2 Stationary-type antenna

For the stationary-type antennas, the results gathered from the inhibition and the asynchronous tests are shown in Figure A.26. No EMI was observed for any ICD.

At the highest sensitivity, the total affected mode number and *P* were 19 and 2,7%, respectively. The worst MID was 15 cm in the inhibition tests, and 2 cm in the asynchronous tests.

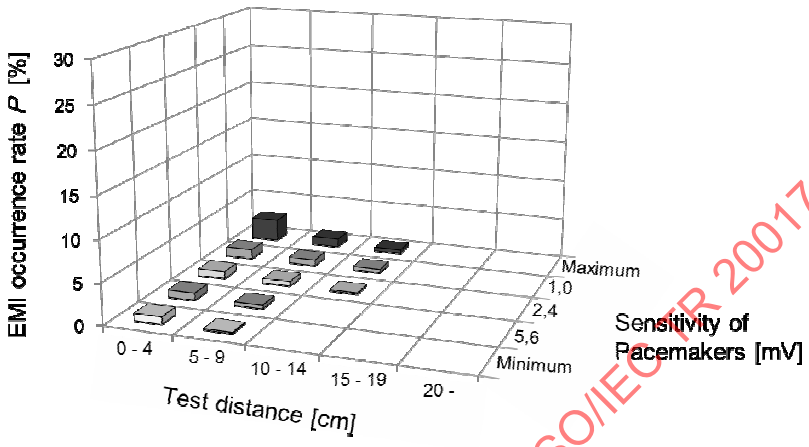

Figure A.26 — Test results of ISO/IEC 18000-3, Mode 1 stationary type RFID interrogators and pacemakers (Inhibition and asynchronous tests at different sensitivities)

A.10.2.3 Gate-type antenna

For the gate-type antennas, the results gathered from the inhibition and the asynchronous tests of pacemakers are shown in Figures A.27 for process 2 and A.28 for process 3 (see Annex A.8).

During test process 1, no EMI was observed.

From Figure A.27 (process 2), at the highest sensitivity and the distance within 4 cm, the total affected mode number and *P* were 2 and 1,7%, respectively. In addition, the worst MID in the asynchronous tests was 23 cm for a pacemaker.

From Figure A.28 (process 3), the total affected mode number and *P* were 10 and 8,3%, respectively. The worst MID in the asynchronous tests was 18 cm for one pacemaker.

The results of ICDs tests are shown in Figure A.29 for “pacemaker function” and Figure A.30 for “defibrillator function”. During test processes 1 and 2, no EMI was observed.

From Figure A.29, the total affected mode number and *P* were 1 and 3,8%, respectively. The worst MID in the inhibition tests was 4 cm for an ICD.

From Figure A.30, the total affected mode number and *P* were 1 and 4,0%, respectively. The worst MID in the false positive tests was 3 cm for an ICD.

As described in Annex A.10.1, the EMI of AIMDs depends on the magnetic flux distribution generated by HF band RFID interrogators. With respect to this mechanism, the numerical estimation method described in Annex A.11, together with a worked example, is effective.

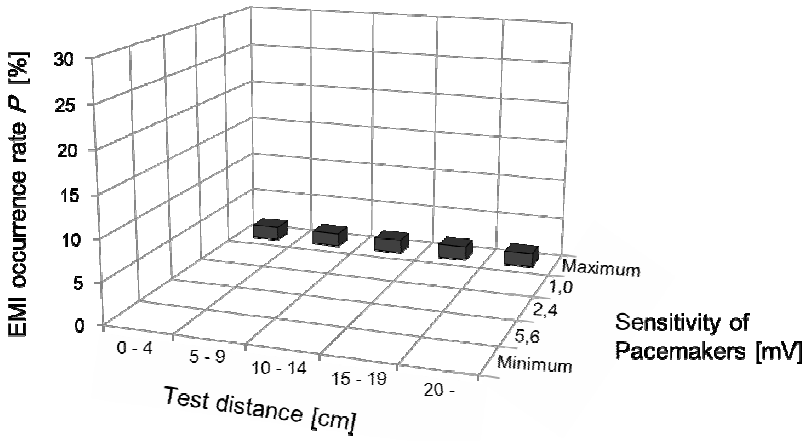

Figure A.27 — Test results of ISO/IEC 18000-3, Mode 1 gate type RFID interrogators and pacemakers (Inhibition and asynchronous tests at different sensitivities, process 2)

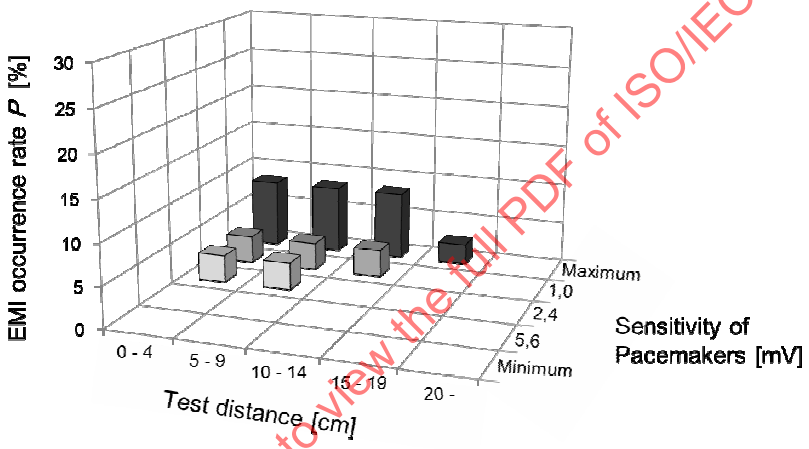

Figure A.28 — Test results of ISO/IEC 18000-3, Mode 1 gate type RFID interrogators and pacemakers (Inhibition and asynchronous tests at different sensitivities, process 3)

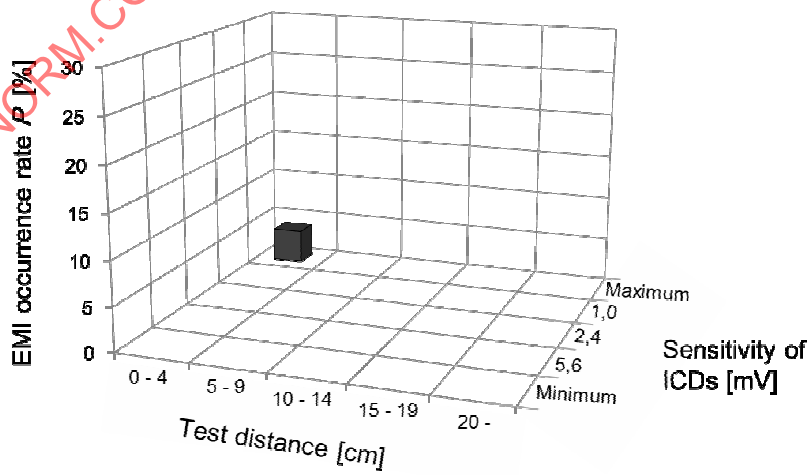

Figure A.29 — Test results of ISO/IEC 18000-3, Mode 1 gate type RFID interrogators and ICDs (Inhibition and asynchronous tests at different sensitivities, process 3)

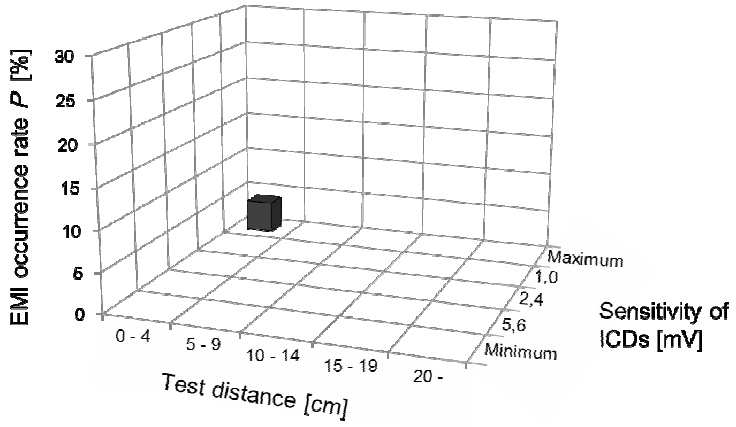

Figure A.30 — Test results of ISO/IEC 18000-3, Mode 1 gate type RFID interrogators and ICDs (False positive and false negative tests at different sensitivities, process 3)

A.10.3 ISO/IEC 18000-4, Mode 1

Four different types of RFID interrogators of the Mode 1 specified by ISO/IEC 18000-4 [4] were tested; their technical information details are in Table A.6. 19 different types of pacemakers and 8 ICDs were used and tests were conducted with various AIMD operation parameter settings, see Table A.4. 304 total measurements were taken. The result was that no EMI was observed for any AIMD.

Table A.6 — RFID interrogators tested (ISO/IEC 18000-4, Mode1)

Frequency	2,45 GHz
Transmission method	Radio wave
Antenna input power	300 mW, 10 mW/MHz
Maximum communication distance guaranteed	~1,5 m ~30 cm
Modulation	Amplitude shift keying (100%)
Air interface protocol	Mode 1
Bit rate	20 kbit/s to 40 kbit/s
Transmission mode	Intermittent
Application type	Stationary
Number of devices	2 (300 mW), 2 (10 mW/MHz)
RF Usage of Intermittent wave (Pulse period, Pulse width)	(160~560 ms, 40 ms)
Antenna size	8,7 × 8,7 × 1,5 cm^3
Transmission polarization	Circular polarization

A.10.4 ISO/IEC 18000-6, Type C (Baseband, Miller subcarrier)

9 different types of RFID interrogators specified by ISO/IEC 18000-6, Type C [5] (EPCglobal Class 1, Generation 2 [10]) were tested, whose technical details are listed in Table A.7. A total of 37 AIMDs were examined, and are listed in Table A.4. The total test practice number was 472 for the Miller subcarrier, intermittent transmission signal, 184 for the Miller subcarrier, continuous transmission signal, and 296 for the baseband, intermittent transmission signal RFID interrogators.

Table A.7 — RFID interrogators tested (ISO/IEC 18000-6 Type C, Baseband, Miller subcarrier)

Frequency	952-954 MHz
Transmission method	Radio wave
Antenna input power (EIRP)	1 W (4 W)
Maximum communication distance guaranteed	~5 m
Modulation	Amplitude shift keying (80% to 100%)
Air interface protocol	Type C
Bit rate	26,7 kbit/s to 128 kbit
Application type	Stationary
Number of devices (Signal type, Transmission mode)	5 (Baseband, Intermittent), 1 (Miller subcarrier, Continuous), 3 (Miller subcarrier, Intermittent)
RF Usage of Intermittent wave (Pulse period, Pulse width)	Baseband: (120 ms, 40 ms), (71,4 ms, 12,1 ms), (200 ms, 40 ms), (260 ms, 39 ms), (360 ms, 39,6 ms) Miller subcarrier: (590 ms, 76,7 ms), (25 ms, 21,5 ms), (278 ms, 180 ms)
Antenna size	Baseband: All are about 20 × 20 × 4 cm^3 Miller subcarrier: All are about 22,5 × 22,5 × 5 cm^3
Transmission polarization	Circular polarization

A.10.4.1 Miller subcarrier, intermittent transmission mode

The test results of UHF RFID interrogators with Miller subcarrier, intermittent transmission signal is shown in Figure A.31. This figure shows test results for pacemakers including cardiac resynchronization therapy-pacemakers (CRT-Ps). There are three RFID interrogator antennas. At the highest sensitivity, the total affected mode number and *P* are 26 and 5,5%, respectively. In addition, the worst MID is 75 cm for inhibition tests and 47 cm for asynchronous tests. These results were observed with only one pacemaker, and with regard to other AIMDs the MIDs were less than 22 cm in all cases. No EMI was observed for ICDs including cardiac resynchronization therapy-defibrillators (CRT-Ds).

There is the possibility that the EMI mitigation filter did not function well at some frequencies in the UHF band with the pacemaker of the worst MID in these experiments, while in the report [38] the feed-through filter effectively rejected the UHF disturbances and thus no EMI was observed.

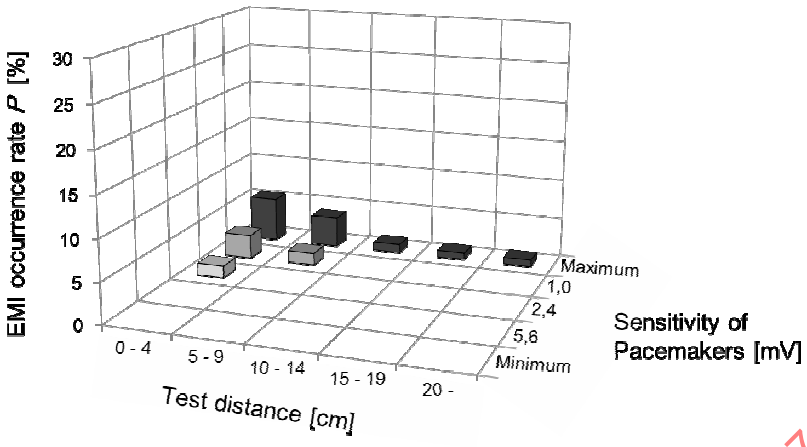

Figure A.31 — Test results of ISO/IEC 18000-6, Type C RFID interrogators with Miller subcarrier-intermittent transmission and pacemakers (Inhibition and asynchronous tests at different sensitivities)

A.10.4.2 Miller subcarrier, continuous transmission mode

The test results of UHF RFID interrogators with Miller subcarrier, continuous transmission signal is shown in Figure A.32. This figure shows test results for pacemakers including CRT-Ps. There is one RFID interrogator antenna. At the highest sensitivity, the total affected mode number and *P* were 6 and 3,3%, respectively. In addition, worst MID was 9 cm for inhibition tests. EMI was not observed in any asynchronous test. Only one pacemaker was affected. No EMI was observed for ICDs, including CRT-Ds.

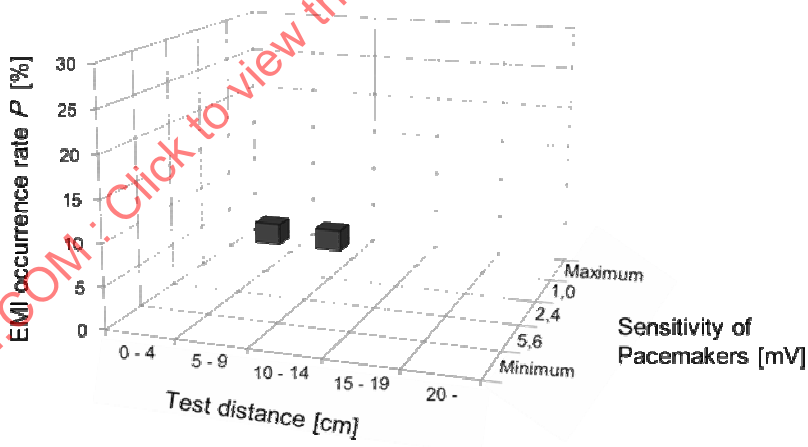

Figure A.32 — Test results of ISO/IEC 18000-6, Type C RFID interrogators with Miller subcarrier-continuous transmission and pacemakers (Inhibition and asynchronous tests at different sensitivities)

A.10.4.3 Baseband, intermittent transmission mode

The test results of UHF RFID interrogator (baseband, intermittent transmission) signals are shown in Figure A.33. This figure shows test results for pacemakers including CRT-Ps. There were five RFID interrogator antennas. At the highest sensitivity, the total affected mode number and *P* were 8 and 2,7%, respectively. In addition, worst MID was 71 cm for inhibition tests and 41 cm for asynchronous tests. No EMI was observed for ICDs including CRT-Ds.

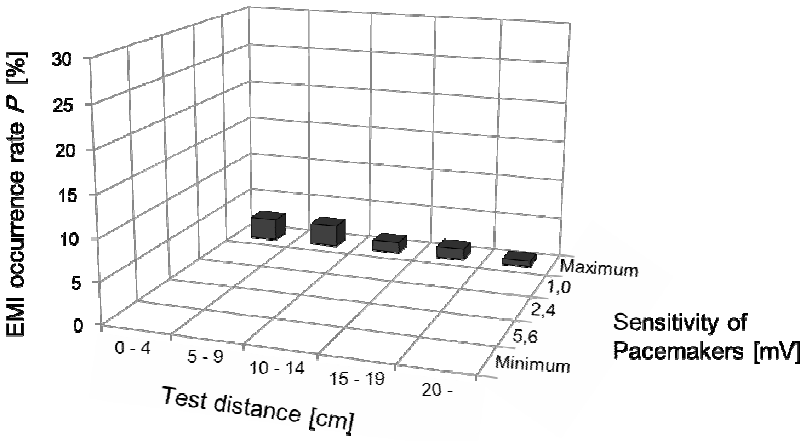

Figure A.33 — Test results of ISO/IEC 18000-6, Type C RFID interrogators with baseband intermittent transmission and pacemakers (Inhibition and asynchronous tests at different sensitivities)

A.10.4.4 Summary

EMI tests using the combination of 9 types of UHF RFID interrogators (Stationary-type) and 37 types of AIMDs (25 types of pacemakers and 12 types of ICDs) were carried out. The most significant effect is complete omission of pacing pulse and continuous generation of asynchronous pulses. However, no EMI was observed for ICDs. With respect to electronic circuit devices and construction, high power handling types are required for ICDs, while pacemakers use low power ones. This difference might be a reason for the differences in EMI seen between ICDs and pacemakers. Detailed investigations of the EMI mitigation filter and the AIMD circuit are expected to find the definitive cause.

The worst MID was 75 cm for just one pacemaker and one RFID interrogator. With another interrogator, 72 cm was obtained. Though it was not confirmed, there is the possibility that the EMI mitigation filter did not function well at some frequencies in the UHF band for the pacemaker with the worst MID. Other pacemakers showed distances less than 20 cm. These values were observed when the pacemaker was set at the maximum sensitivity. The MID was drastically shortened when the sensitivity was reduced. RFID interrogators with intermittent transmission signals tend to significantly impact AIMDs. This is because these periods match the physiological periods of human heartbeat (few Hz to several hundred Hz).

A.11 EMI evaluation method based upon numerical simulations

A novel numerical RFID/AIMD-EMI estimation methodology based upon FDTD analysis is presented here [33]~[35]. This assessment methodology can be applied to ISO/IEC 18000-2 Type A and -3 ISO/IEC Mode 1. Here, an example for ISO/IEC 18000-3 Mode 1 in the frequency band of 13,56 MHz, is introduced. It assumes that RFID interrogators operating in the low or HF frequency bands might cause EMI on the AIMDs through the interference voltage induced by the magnetic flux excited by the RFID interrogator.

First, a numerical HF RFID interrogator antenna model and a human torso phantom model were constructed. Second, the measured and calculated magnetic field distributions generated around an antenna were compared to confirm the validity of the numerical antenna model. Next, interference voltage induced at the connector of the pacemaker was calculated based upon the FDTD method. Finally, to validate the analysis result, the calculated interference voltage was compared with the EMI characteristics obtained by in-vitro EMI experiments.

Numerical models of the HF RFID interrogator single-loop antennas and a human torso phantom were constructed. To obtain the desired resonance frequency and near field characteristic, a parallel capacitance was connected to the antenna coil. FDTD analyses of numerical models were conducted by using EMF simulation software based on the FDTD method, as one example; [54]. Figure A.34 shows an example of calculated example of antenna input impedance. As shown in the figure, the parallel resonance of the antenna was confirmed to occur at 13,56 MHz. In addition, the human torso phantom model, which contains the implantable-cardiac pacemaker model, is shown in Figure A.35. The torso phantom employed for the in-vitro EMI experiments is a modification of Irnich's model as described in Annex A.6. This human torso phantom is composed of an acrylic tank filled with saline solution (1,8 g/l). The dielectric constant and the electric conductivity of each material at 13,56 MHz were input to the model. The coaxial lead wires, which sense the human heart beat signal and stimulate the cardiac muscle, were connected to the pacemakers' terminals. The interference voltage was evaluated at these terminals.

In order to estimate the validity of this simulation method, experimental HF RFID interrogator antennas were constructed. These antennas have the same dimensions as the numerical models. Figure A.36 is a picture of a fabricated antenna that consists of a single turn copper coil and a matching circuit; the coil's dimensions were 300 mm × 300 mm (width × height). Their return loss was more than -20 dB at 13,56 MHz.

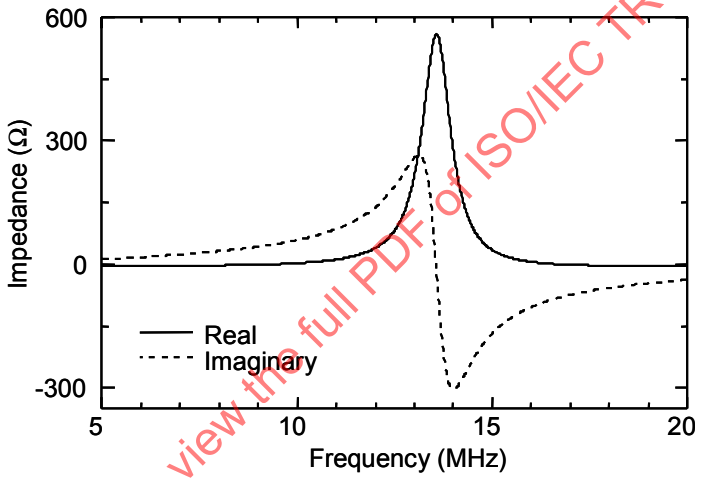

Figure A.34 — Input antenna impedance of 13,56 MHz numerical model

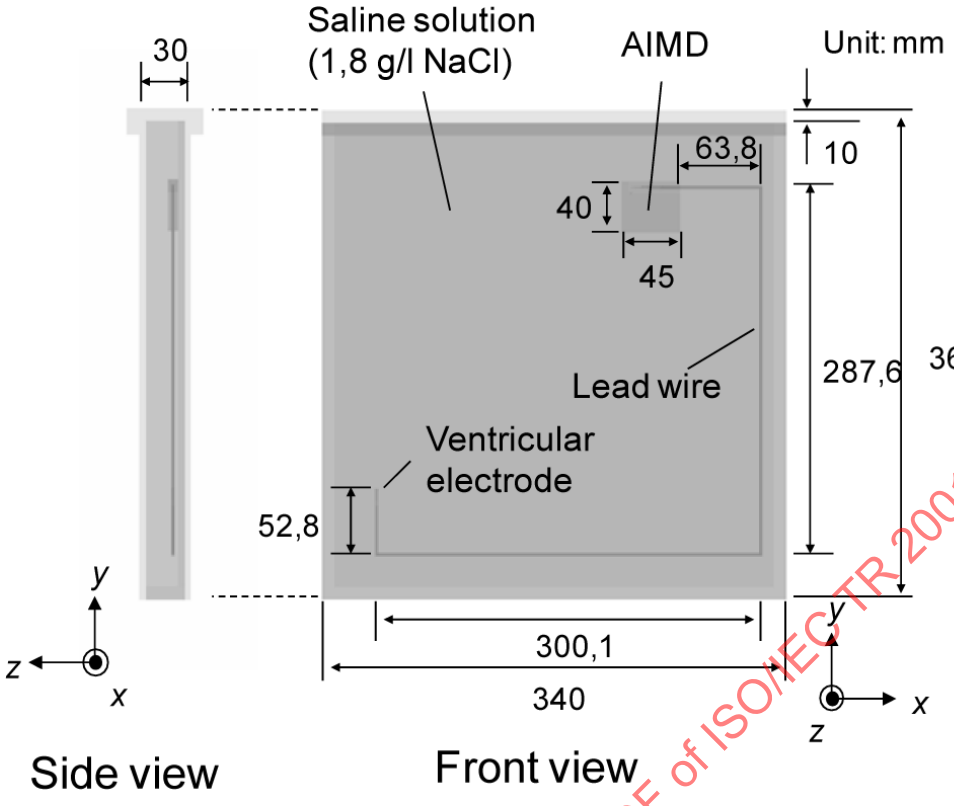

Figure A.35 — Numerical torso phantom with AIMD model

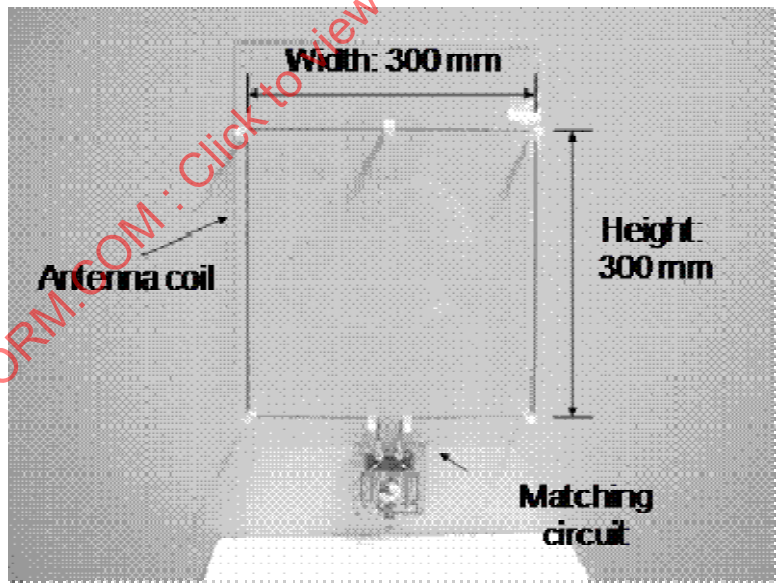

Figure A.36 — 13,56 MHz antenna model for experimental validation

The magnetic field distribution was measured in detail using a three-dimensional automatic field measurement system. The overall view of the measurement setup is shown in Figure A.37. These measurements used a magnetic field probe [52]. Figures A.38a and A.38b show the two-dimensional magnetic field strength of the measured and calculated values, respectively. These values are magnetic field strengths at the surface of the antenna (xy-plane shown in Figure A.39) and are normalized against the maximum values. The calculated values agree well with the measured values.

The interference voltage induced at the connector of the pacemaker was similarly calculated based upon the FDTD method. As shown in Figure A.39, the antenna model and the human torso phantom model are combined to obtain the interference voltage. The antenna is located so that the centre of the antenna coil and the centre of the human torso phantom lie on the same axis. The voltage is evaluated at both ends of the resistor connected to the terminal. In the analysis, 1 MΩ was large enough to obtain a stable computed voltage.

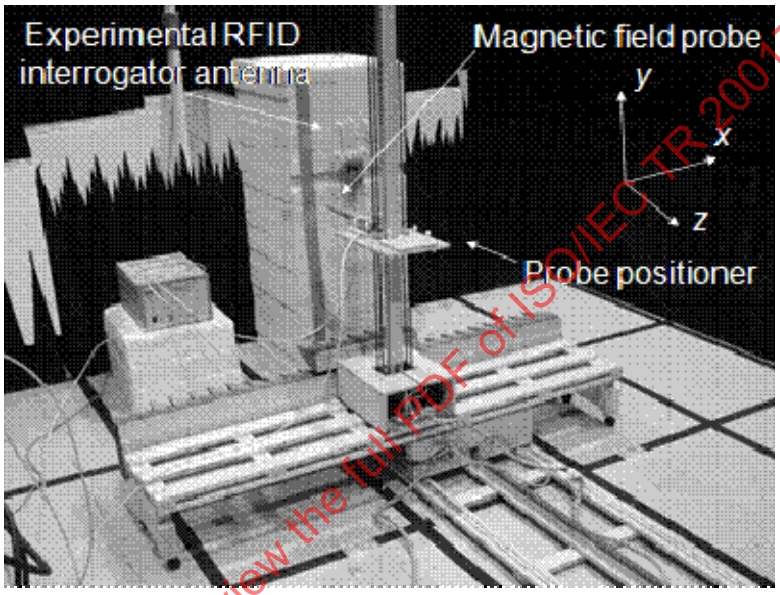

Figure A.37 — 3-D Measurement system for 13,56 MHz magnetic field distribution near antenna

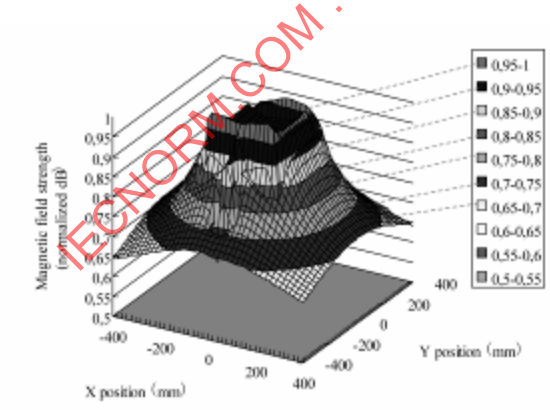

Figure A.38a — Measured

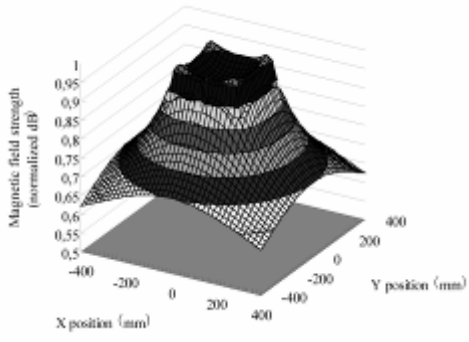

Figure A.38b — Calculated

Figure A.38 — 13,56 MHz magnetic field distribution near antenna

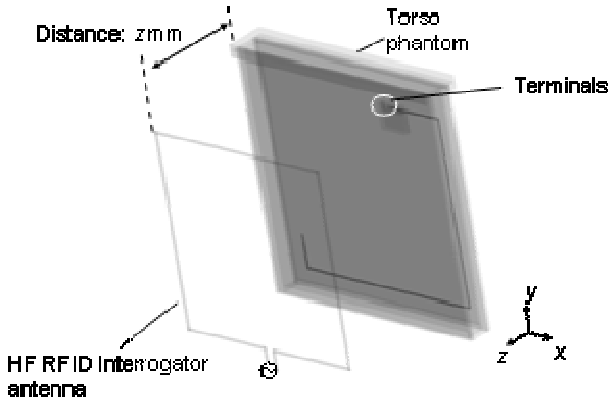

Figure A.39 — Spatial arrangement of antenna and torso models

Figure A.40 shows the normalized induced voltage at the terminal versus distance z from the surface of the RFID interrogator reader/writer antenna model. The input powers of the two antennas were the same. The induced voltages for two different antenna sizes are shown as well. Antenna A has a large coil, 300 mm × 300 mm (width × height). Antenna B has a relatively small coil, 200 mm × 200 mm (width × height). When distance z is 0 cm, the induced voltage of antenna A is more than twice that of antenna B, even though its input power is the same. This is because the difference in magnetic field distribution strongly influences the induced voltage, rather than the maximum magnetic field strength at one point [34]. By using the FDTD method to evaluate the interference voltage, precise and accurate estimation can be achieved.

In order to validate the analysis result, the calculated interference voltage was compared to the EMI characteristics obtained by in-vitro EMI experiments. The in-vitro EMI experiments were conducted using the fabricated antennas described above. In the experiments, pacemaker malfunctions such as omission of pacing pulses or the generation of asynchronous pulses were identified and recorded. The positions of the antenna and the human torso phantom were set to be the same as in the analysis. The MID was measured and recorded.

Figure A.41 shows the MIDs versus the antenna input power. The solid and dashed lines show the analyzed results of each antenna based upon the FDTD method. These lines show the shortest distance at which the interference voltage exceeds the specific threshold voltage. The threshold voltage was experimentally obtained using a susceptible pacemaker and estimations were made on this pacemaker. In addition, the closed circles and the closed triangles indicate the MIDs obtained in the experiments. As shown in the figure, the calculated results agree very well with the experimental results.

More information is given in the references [33]~[35].

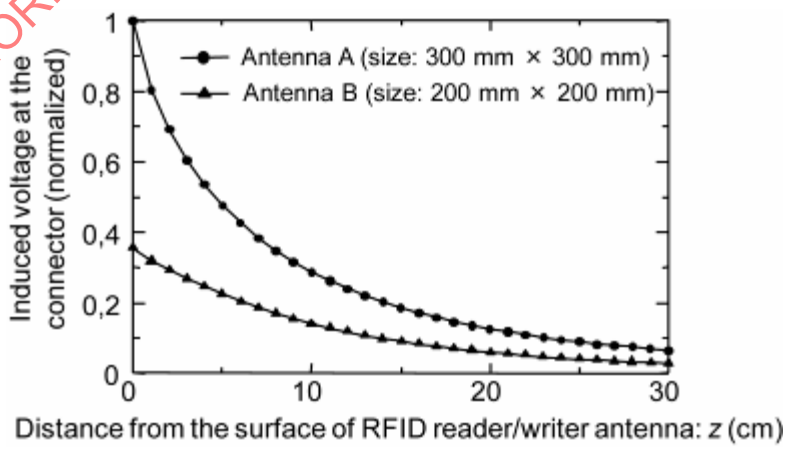

Figure A.40 — Calculated terminal voltage versus distance between antenna and phantom

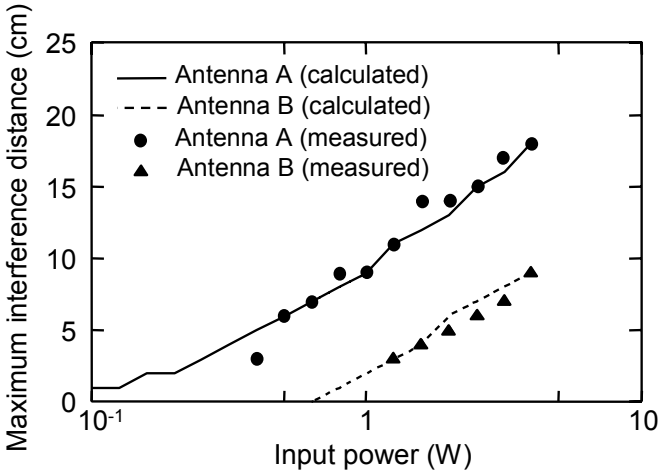

Figure A.41 — Predicted and measured MIDs versus antenna input powers

A.12 Radio filler technique

A.12.1 Principle of radio filler

The following details a radio filler technique that mitigates the noise associated with amplitude and pulse modulation that can affect AIMDs. Note that neither frequency nor phase modulation produce the noise issues and thus can be used without the need for mitigation techniques.

The literature predicts that the principal RF interaction in AIMDs is spurious EMI signal generation through undesired demodulation of high amplitude RF signals on pacing leads [25], [29], [30], ANSI/AAMI PC69. In addition, an important mechanism is speculated to be the envelope demodulation phenomenon that occurs at the overvoltage protection diodes and/or the first stage sensing amplifier [25], [30], [36], [53]. The spurious components include very low frequencies and other such frequency combinations that generate low frequency inter-modulation products. From these, it can be suggested that a constant envelope RF signal is unlikely to impose any significant EMI on AIMDs. This is because a constant envelope signal cannot generate noise through the envelope demodulation behaviour of the non-linear devices in the AIMDs.

Many RFID systems transmit signals intermittently at regular periods. The idle period can range from 10 to 500 ms depending on the system. The difference in field strength between the transmitting time and the idle time causes pulse shaped envelope variations and thus low frequency noise signals are created in the AIMDs.

"Radio filler", the EMI mitigation method proposed here, is based on a "mitigation signal" that lies within the idle periods of the transmission signal. The radio filler, sent from the same or a different antenna, suppresses the time variation in the envelope curve. This reduces the low frequency noise signals generated by the nonlinear characteristics of the AIMDs' internal circuits, and so drastically improves the MID. This expectation is true for practical systems and the argument is as follows; the RFID burst signal is modulated by techniques such as amplitude-shift keying, frequency-shift keying, and Gaussian minimum-shift keying [13]. However, since the modulation period is generally small compared to the non-modulated (constant envelope) period in a burst, burst signals of RFID interrogators might be regarded as constant envelope-like signals as a whole. Moreover, data transmission between RFID interrogators and passive tags is realized by using modulated backscattering or load modulation [13]. Because of this, data transmission is completed in one burst signal. Therefore, the filler signal in the idle periods does not interfere with tag communication. In addition, modulation schemes such as amplitude-shift keying in the RFID signal usually employ modulation frequencies above 10 kHz. This suggests that even if these signals are demodulated by the nonlinear characteristics of AIMDs, the dominant part of these signals cannot pass into the sensing circuits of the AIMDs.

A simplified structure of the filler signal is shown in Figure A.42. It is clear that both the frequency and amplitude of the radio filler burst signal should match those of the transmitting signal to achieve high mitigation performance. In practical operations, however, some deviations both in frequency and amplitude are permitted; details are experimentally estimated in A.12.3.

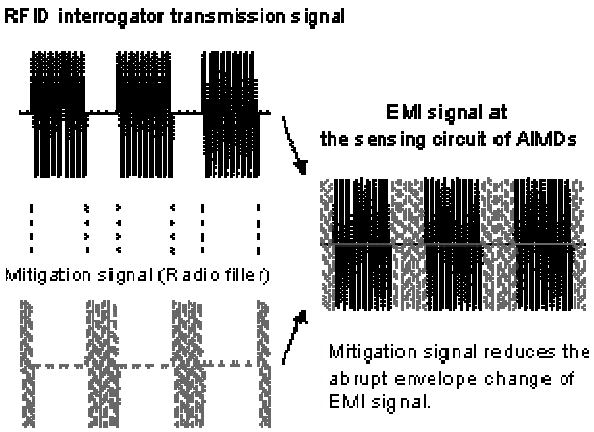

Figure A.42 — Fundamental structure of mitigation signal

A.12.2 Experimental set-up

In order to evaluate the radio filler technique, some in vitro EMI experiments were carried out. Among the various AIMDs tested in Annex A.10, four types of actual pacemakers were used as typical low immunity AIMDs. To obtain sufficiently conservative EMI test results, the sensitivity and refractory period of the pacemakers were set at maximum (most sensitive) and minimum, respectively. The stimulation mode was programmed to AAI or VVI. Sensing and pacing polarity were either unipolar mode or bipolar mode.

Figure A.43 shows the type-A experimental set-up to estimate the basic performance of the radio filler technique. Two RF signal generators and a standard dipole antenna for each test frequency band were used to simulate an RFID interrogator. A single-carrier continuous pulse train signal was used to simulate the RFID signal. The radio filler was transmitted by the same antenna as used for the RFID signal. The output signals of two signal generators were combined in a hybrid and radiated by a standard dipole antenna. One signal generator output an intermittent signal A representing the RFID interrogator signal. The other generator output the radio filler signal $\overline{A}$. This set-up can yield experiments on frequencies from 450 MHz up to 1 000 MHz.

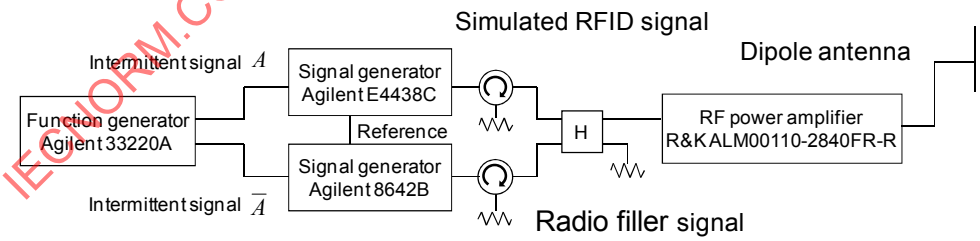

Figure A.43 — Type-A experimental set-up for estimating fundamental mitigation effects by radio filler technique

Figure A.44 shows an overview of the measurement set-up of the radio filler mitigation method experiments. In the experiments, the human torso phantom faced a dipole antenna. Figures A.45 and A.46 show measured waveform examples of the RFID interrogator signal *A* and the radio filler signal $\overline{A}$. In this case, the RFID interrogator signal and radio filler had frequencies of 950 MHz and 850 MHz, respectively. From these, radio filler signals acted to fill the signal gaps between RFID interrogator signal bursts while keeping the phase

continuous connection (Figure A.46). This is because the phase continuous connection suppresses the generation of undesirable demodulation components at the transition of the two signals and so yields better mitigation performance.

The periods of these signals were controlled by an external function generator. In the experiments, the frequency spacing between the RFID signal and the filler signal was changed to confirm the mitigation effect.

Figure A.47 shows the type-B experimental set-up which used actually modulated RFID interrogator signals. The output signals of a UHF RFID interrogator and the signal generator were combined in a hybrid and radiated by the same dipole antenna. The signal of the RFID interrogator was demodulated by a carrier sense unit and used to control the signal generator. Type-B set-up was constructed to confirm mitigation performance with actual RFID interrogator signals (UHF) and 13,56 MHz RFID interrogators.

The antenna input power was adjusted to 1 W for all tests.

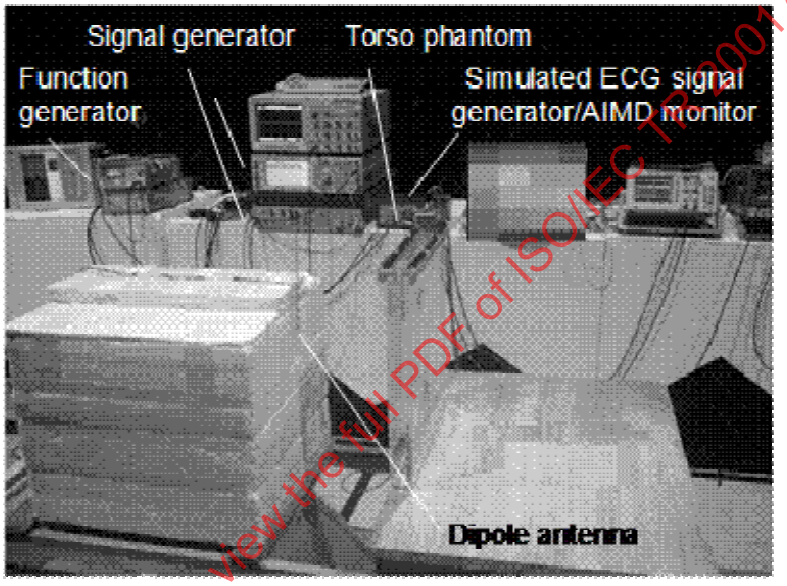

Figure A.44 — Experimental set-up to estimate radio filler method

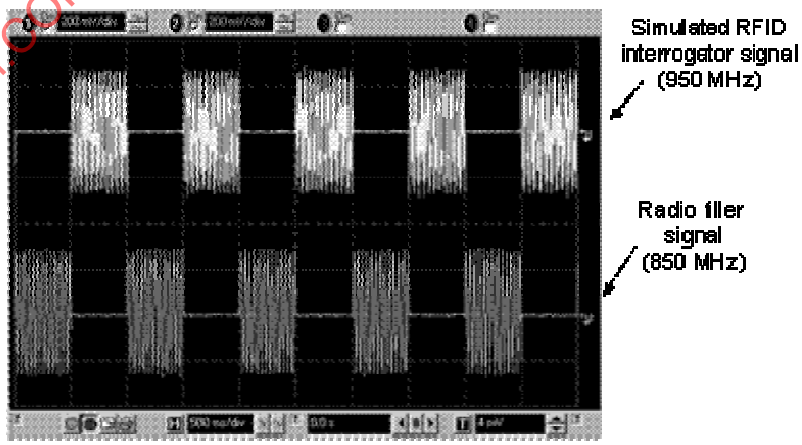

Figure A.45 — Waveforms of RFID interrogator and Radio filler signals